# Komatiites I: Eruption and Flow

*by* HERBERT E. HUPPERT[1] AND R. STEPHEN J. SPARKS[2]

[1]*Department of Applied Mathematics and Theoretical Physics, University of Cambridge, Silver Street, Cambridge CB3 9EW*

[2]*Department of Earth Sciences, University of Cambridge, Downing Site, Cambridge CB2 3EQ*

(*Received 18 June 1984; revised typescript accepted 17 December 1984*)

## ABSTRACT

Because of their high eruption temperatures and ultrabasic composition, komatiite lavas had low viscosities, which typically ranged from 0·1 to 10 Pa s. A major consequence of this low viscosity is that most lavas erupted as turbulent flows. An analysis of their ascent through the lithosphere suggests ascent velocities in the range of 1 to over 10 m $s^{-1}$ and Reynolds numbers much greater than the critical value of 2000. The lavas would have remained turbulent for most or all of their subsequent flow and emplacement. Typical horizontal flow rates are estimated to range from 0·5 to 100 $m^2$ $s^{-1}$ per unit width of flow. Such turbulent lava flows would have lost their heat by convection to the surroundings, at rates which are orders of magnitude greater than the rates for laminar flows, which cool by conduction. A quantitative analysis of the cooling of komatiites indicates cooling rates from over 1000 °C $hr^{-1}$ to a few °C $hr^{-1}$, while the flows remained turbulent. These rates are in an appropriate range to cause phenomena such as high nucleation rates, strong supersaturation of the lava, delayed nucleation of olivine, and skeletal or dendritic crystal morphologies.

Komatiites often flowed over ground composed of rocks with lower melting temperatures. It is proposed that the turbulent lavas melted the ground to form deep thermal erosion channels. Melting rates at the lava source are calculated at several metres per day, and deep troughs with depths of several metres to hundreds of metres and lengths of several kilometres probably formed. Laboratory experiments performed to simulate thermal erosion show qualitative agreement with the theory with channel depth decreasing downstream. The experiments also revealed that the channel margins become undercut during thermal erosion to form overhanging sides of the channel. Some sinuous rilles observed in the mare regions of the Moon are thought to have formed by thermal erosion (Hulme, 1973). They provide analogues of the channels postulated to form in komatiite eruptions, where conditions were in fact more favourable for thermal erosion. An assessment of the role of olivine crystals, precipitated in the cooling, turbulent flows, indicates that they will remain in suspension until the lava has come to rest.

Contamination of komatiite lava by underlying rock can be as much as 10 per cent. Some illustrative calculations show how the major element and trace element compositions of residual melts can be significantly modified by combined assimilation and fractional crystallization in a moving flow. Assimilation of tholeiitic basalt into a komatiite can cause incompatible trace element ratios, such as Ti/Zr and Y/Zr, and the rare earth patterns of derivative lavas, to vary substantially. Some of the variations in such geochemical parameters, which are often ascribed to mantle heterogeneity, also could have resulted from assimilation of the ground. Assimilation could have modified the isotope geochemistry of lava suites and led to apparent ages which differ from the true eruption age. The thermal erosion model also provides an explanation of the formation of some nickel sulphide ores found at the bottom of thick komatiite flows. It is proposed that ores can form by assimilation of sulphur-rich sediment, which combines with Ni from the komatiite to form an immiscible liquid.

[Journal of Petrology, Vol. 26, Part 3, pp 694–725, 1985]

© Oxford University Press 1985

Downloaded from http://petrology.oxfordjournals.org at Cambridge University on July 19, 2010

## SYMBOLS

| *Letters* | *Meaning* | *Defined* | *Value* |
|---|---|---|---|
| *Roman* | | | |
| $A$ | cross-sectional area of fluid-filled crack | | |
| $c_g$ | specific heat of ground | | 730 J kg$^{-1}$ °C$^{-1}$ |
| $c_l$ | specific heat of komatiite lava | | 730 J kg$^{-1}$ °C$^{-1}$ |
| $D$ | a constant | (15) | |
| $d$ | fissure width | | |
| $E$ | a constant | (16) | |
| $F$ | a constant | (18) | |
| $G$ | shear modulus | | |
| $g$ | acceleration due to gravity | | 9·81 m s$^{-2}$ |
| $H$ | heat transfer rate from komatiite to ground | | |
| $h$ | thickness of komatiite flow | (9) | |
| $h_T$ | heat transfer coefficient | (12) | |
| $\bar{h}_T$ | heat transfer coefficient modified to account for crystallization | (19) | |
| $K$ | a constant | (1) | 1·67 |
| $k$ | friction coefficient | (8) | 0·03 |
| $k_l$ | thermal conductivity for komatiite lava | | 1 W m$^{-1}$ °C$^{-1}$ |
| $L_c$ | length of fluid-filled crack | (4), (5) | |
| $L_g$ | latent heat for melting of ground | | $8 \times 10^5$ J kg$^{-1}$ |
| $L_x$ | latent heat for crystallization in komatiite lava | | $8 \times 10^5$ J kg$^{-1}$ |
| $P_0$ | representative magma pressure | | |
| $Pr$ | Prandtl number of komatiite lava $= c_l \mu_2 / k_l$ | | |
| $Q$ | two-dimensional flow rate | (6) | |
| $Re$ | Reynolds number $= Q/v$ | (7) | |
| $S$ | amount of assimilated ground expressed as a volume fraction | (22) | |
| $T$ | temperature | | |
| $T_f$ | freezing temperature of komatiite lava | | 1200 °C |
| $T_l$ | temperature of komatiite lava | | |
| $T_m$ | melting temperature of ground | | 850–1200 °C |
| $T_0$ | initial temperature of ground and overlying sea water | | 0 °C |
| $u$ | velocity of komatiite lava flow $= Q/h$ | | |
| $V$ | velocity of ground/melt interface | (10) | |
| $V_*$ | shearing stress velocity | (23) | |
| $v$ | vertical velocity of komatiite magma in fissure $= Q/d$ | | |
| $x$ | fractional crystal content | | |
| $x_m$ | distance from source where the lava temperature equals the melt temperature of the ground | (21) | |
| *Greek* | | | |
| $\beta$ | a constant | | 0·3 |
| $\gamma$ | a constant | (17) | |
| $\theta$ | temperature of komatiite lava in excess of the melting temperature of the ground | (11) | |
| $\theta_0$ | (initial) value at source of $\theta$ | | |
| $\mu_1$ | dynamic viscosity of komatiite liquid | (2) | |
| $\mu_2$ | dynamic viscosity of komatiite liquid plus crystals | (3) | |
| $\mu_D$ | shear viscosity of crystal/liquid mixture | (1) | |
| $\mu_L$ | dynamic viscosity of liquid | | |
| $\nu$ | kinematic viscosity of komatiite magma | | |
| $\Delta\rho$ | density difference between komatiite magma and lithosphere | | 100–300 kg m$^{-3}$ |
| $\delta\rho$ | density difference between komatiite lava and overlying sea water | | 1800 kg m$^{-3}$ |
| $\rho$ | mean density of lithosphere | | |

Downloaded from http://petrology.oxfordjournals.org at Cambridge University on July 19, 2010

| *Letters* | *Meaning* | *Defined* | *Value* |
|---|---|---|---|
| *Greek (cont.)* | | | |
| $\rho_l$ | density of komatiite lava | | 2800 kg m$^{-3}$ |
| $\rho_m$ | density of komatiite magma | | 2800 kg m$^{-3}$ |
| $\rho_g$ | density of ground | | 2700 kg m$^{-3}$ |
| $\sigma$ | Poisson's ratio | | |
| $\sigma_1 - \sigma_3$ | deviatoric stress in the lithosphere | | 10–20 MPa |
| $\sigma_3$ | minimum stress | | |

## 1. INTRODUCTION

Komatiite lavas were erupted predominantly during the Archaean. They provide potential information on the thermal conditions of the early Earth, on the composition of the Archaean mantle, and on ancient volcano-tectonic processes. They can also be host to important nickel sulphide mineralization and often display spectacular textural and compositional layering. Part I of our study presents a detailed analysis of their eruption and flow, using volcanological arguments and fluid dynamical principles. Part II analyses the processes of crystallization and cooling after emplacement. A brief description of the main ideas was presented by Huppert *et al.* (1984).

There are many problems in attempting an analysis of komatiite eruptions. Most of these rocks have been metamorphosed and deformed. Primary volcanic features can be obscured by later tectonic and metamorphic modifications. There have only been a few studies of well-exposed and well-preserved lavas, such as at Munro Township, Ontario (Pyke *et al.*, 1973). Much of the background normally available to the volcanologist, such as typical flow volumes, vent geometry and location, depth of magma origin and tectonic environment, is lacking or contentious. No data are available on the size, style or duration of komatiite eruptions. In these circumstances, theoretical analysis of the major physical processes in komatiite eruptions can provide an important framework within which to understand the geology, geochemistry, and petrology of the komatiites.

In Section 2 we discuss the rheological properties of komatiites. In Section 3 we consider the ascent of komatiite magma through the lithosphere and place constraints on magma volumes and eruption conditions at the vent. For a wide range of magma volumes and ascent rates, komatiites are likely to emerge from the vent as fully turbulent flows. In Section 4 we analyse the flow and cooling of komatiite lava. We examine the idea that komatiites will melt and assimilate the underlying ground to form deep, thermal erosion channels. Some laboratory experiments, in which hot water was discharged over a slab of polyethylene glycol, are also described to illustrate the process of thermal erosion. The influence of crystallization on flow behaviour is also considered. In Section 5 we consider the geological and geochemical implications of assimilation for incompatible trace element and isotopic variations within komatiite suites. We also argue that nickel-sulphide mineralization in komatiites could have been caused by assimilation of sediment.

## 2. RHEOLOGICAL PROPERTIES OF KOMATIITES

No laboratory measurements of viscosity have been made on liquids of komatiite composition. Use of the empirical methodologies of Shaw (1972), Bottinga & Weill (1972), and Urbain *et al.* (1982) for komatiites is complicated by the fact that the empirical coefficients have largely been estimated from experimental data on silicate liquids at temperatures well below komatiite eruption temperatures and with higher mole fractions of $SiO_2$. The empirical coefficients are consequently rather poorly known for highly magnesian liquids. Komatiites are predominantly composed of $SiO_2$, $MgO_2$ and FeO, which typically

Downloaded from http://petrology.oxfordjournals.org at Cambridge University on July 19, 2010

TABLE 1

*Measured and calculated viscosities of liquids in the $MgO$-$SiO_2$ and $MgO$-$SiO_2$-$Al_2O_3$ systems*

| *Composition* | *Temperature (°C)* | *Viscosity (Pa s)* | | |
|---|---|---|---|---|
| | | *1* | *2* | *3* |
| $MgO = 40\%$; $SiO_2 = 60\%$ | 1600 | 0·32 | 0·12 | 0·37 |
| | 1700 | 0·18 | 0·07 | 0·21 |
| | 1800 | 0·12 | 0·05 | 0·13 |
| $MgO = 15{\cdot}3\%$; $SiO_2 = 45{\cdot}8\%$; $Al_2O_3 = 38{\cdot}9\%$ | 1600 | 1·25 | 0·91 | 1·24 |
| | 1700 | 0·62 | 0·50 | 0·66 |
| | 1800 | 0·53 | 0·29 | 0·37 |

1. Viscosities measured in experiments of Urbain *et al.* (1982).
2. Calculated viscosities using method of Shaw (1972).
3. Calculated viscosities using modified method of Shaw (1972) as detailed in this paper.

constitute 80 to 90 per cent of the total components. New experimental rheology data on melts in the $MgO$-$SiO_2$ and $FeO$-$SiO_2$ systems, which are quite similar to komatiite in terms of temperature and composition, have recently been presented by Urbain *et al.* (1982). However, application of Shaw's (1972) method to the $MgO$-$SiO_2$ system (Table 1) yields measured viscosities which are two to three times greater than the calculated values. The difference becomes even greater at higher temperatures, which indicates that the empirical molar coefficient for MgO chosen by Shaw (1972) is inappropriate for such compositions. We have consequently modified Shaw's method by increasing the partial molar coefficient for MgO from 3·4 to 4·0, but we have maintained the coefficient for FeO at 3·4. This procedure produces calculations for both $MgO$-$SiO_2$ and $FeO$-$SiO_2$ liquids which closely agree with the laboratory measurements. The modification makes only minor differences to the viscosities estimated for other kinds of lavas, since MgO makes only a relatively small contribution to the viscosity.

Crystallization can subsequently increase viscosity by changing the composition of the residual liquid and by introducing dispersed solids. The first effect can be modelled for

TABLE 2

*Compositions of komatiitic liquids used in modelling viscosity variations in komatiites. Successive compositions define a liquid line of descent. The liquidus temperature, T, total fraction of olivine crystals present (assuming an initial composition 1), $X_s$, and fosterite content of olivines, Fo, are also indicated*

| | *1* | *2* | *3* | *4* | *5* |
|---|---|---|---|---|---|
| $SiO_2$ | 46·50 | 47·24 | 48·96 | 50·76 | 52·45 |
| $TiO_2$ | 0·19 | 0·22 | 0·28 | 0·34 | 0·40 |
| $Al_2O_3$ | 3·58 | 4·10 | 5·21 | 6·35 | 7·46 |
| FeO | 10·22 | 10·79 | 11·79 | 12·44 | 12·81 |
| MgO | 33·00 | 30·30 | 25·11 | 19·93 | 14·75 |
| CaO | 5·10 | 5·84 | 7·42 | 9·03 | 10·61 |
| $Na_2O$ | 0·49 | 0·56 | 0·71 | 0·86 | 1·01 |
| $K_2O$ | 0·18 | 0·21 | 0·26 | 0·32 | 0·38 |
| $T$ (°C) | 1650 | 1600 | 1500 | 1400 | 1300 |
| $X_s$ | — | 0·127 | 0·312 | 0·435 | 0·519 |
| Fo | — | 93·6 | 92·6 | 90·8 | 89·5 |

Downloaded from http://petrology.oxfordjournals.org at Cambridge University on July 19, 2010

komatiites by calculating a liquid line of descent controlled by olivine crystallization. Table 2 shows a succession of liquids derived from a komatiite with 33 per cent MgO by olivine crystallization. Liquidus temperatures were estimated for each successive liquid using the algorithm recommended by Bickle (1982) linking MgO content with liquidus temperature. The fraction of olivine crystals crystallized at each stage is indicated. Fig. 1 shows the variation of viscosity at the liquidus temperature as a function of MgO content and temperature using the data in Table 2 to define a representative curve for komatiites. Calculations of viscosities for Barberton komatiites (after Smith & Erlank, 1982) fall close to this curve, showing that minor variations in other components ($Al_2O_3$, $TiO_2$, CaO, $Na_2O$) do not strongly affect the viscosity estimates. The calculated viscosity for the same komatiite compositions plus one weight per cent $H_2O$ is slightly lower (Fig. 1).

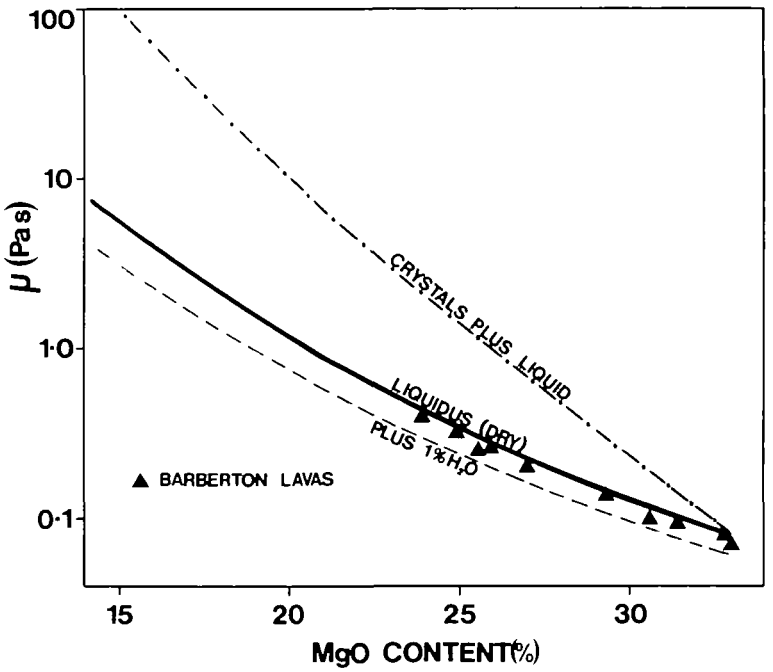


FIG. 1. The viscosity as a function of the melt composition and crystal content. The solid line shows the viscosity of the residual liquids as a function of the MgO content for the liquid line of descent calculated in Table 2. The dashed line shows the effect of having 1·0 per cent $H_2O$ dissolved in the melt. The dot-dash line shows the variation of viscosity with composition for the bulk composition 1 (Table 2) with the assumption that olivine crystals remain in suspension. For this latter case, the composition of residual liquid is plotted against the viscosity of this liquid plus dispersed crystals. The solid triangles plot viscosity estimates for komatiite compositions reported by Smith & Erlank (1982).

The effect of dispersed olivine crystals on viscosity can be approximately estimated from the empirical formula of Ting & Luebbers (1957) for two-phase systems

$$\mu_D = \mu_L(1 - Kx)^{-2\cdot5}, \quad (1)$$

where $\mu_L$ is the viscosity of the liquid, $\mu_D$ is the shear viscosity of the crystal/liquid mixture, $K$ is an empirical constant with value 1·35 for uniform spheres, and $x$ is the volume fraction of crystals. Marsh (1981) has concluded that $K = 1{\cdot}67$ gives better agreement with observed measurements of crystal-rich lavas.

Downloaded from http://petrology.oxfordjournals.org at Cambridge University on July 19, 2010

Fig. 1 shows two curves representing the variations of viscosities of liquid alone and liquid plus crystals for a 33 per cent MgO composition. The variation of viscosity with temperature for the case of liquid alone can be approximated by the following empirical formula

$$\mu_1 = \exp(15{\cdot}095 - 0{\cdot}0104T), \tag{2}$$

where $T$ is in degrees centigrade and viscosity is in Pa s. In Section 4 our model employs the variation of viscosity with decreasing temperature and increasing crystal content of a komatiite whose liquidus temperature is 1650 °C (the dot-dashed line in Fig. 1). With the assumption that all the crystals remain in suspension, the dependence of viscosity on crystal content and temperature can be approximated by

$$\mu_2 = \exp(34{\cdot}551 - 0{\cdot}0226T). \tag{3}$$

## 3. MAGMA GENERATION, ASCENT AND ERUPTION

### *3a. Magma generation and asthenosphere transport*

Surface eruption of liquids with MgO contents of up to 33 per cent requires the mantle to reach its solidus at great depths. Experimental studies of komatiite generation (Bickle *et al.*, 1977) and thermal constraints (McKenzie, 1984) indicate depths of 200 km or greater. If the Archaean upper mantle was broadly similar to that of today, komatiite liquids would need to have been formed by one or more of: high degrees of partial melting; complex polybaric assimilation; sequential melting (Bickle *et al.*, 1977); or by melting at very high pressure (O'Hara, 1968; McKenzie, 1984). The generation and transport of komatiite within the asthenosphere, however, remain controversial and obscure (Nisbet, 1982; Nisbet & Walker, 1982; Jarvis & Campbell, 1983). For present purposes, the komatiite is assumed to accumulate at the base of the lithosphere and then ascend to the surface. There is likely to be a close connection between the rate of accumulation of komatiite at the base of the lithosphere and the frequency of magma ascent, magma volume, and rates of ascent (Shaw, 1980).

### *3b. Lithosphere ascent and magma volumes*

Geological and geophysical evidence indicate that there is a wide spectrum in the style of magma ascent through the modern lithosphere. At one extreme, basalt magma can be transported almost continually from the asthenosphere through mature, long-established conduit systems (Ryan *et al.*, 1981). Crustal magma chambers are established within the system in which extensive differentiation can occur. Lava volumes and eruption rates tend to be small to moderate in such systems (typically $< 1$ km$^3$ and $< 500$ m$^3$ s$^{-1}$ respectively). At the other extreme, large volumes of magma can ascend through the lithosphere from a deep source with no pre-existing channelways established. The deep source may be a sub-crustal magma chamber, or due to the direct segregation of primary magma from a partially melted mantle. The primitive character of komatiite favours a deep origin with rapid transport along new pathways through the lithosphere. Such eruptions in modern volcanic provinces produce monogenetic volcanic structures ranging from large voluminous flood basalts (1–1000 km$^3$), through low-angle shield volcanoes (0·1–10 km$^3$) to small lava fields and associated cinder cones ($< 1$ km$^3$).

The main mechanism of rising fluid magmas through the lithosphere is generally accepted to be by propagation of magma-filled cracks (Shaw, 1980). Analysis of the geometry and propagation of fluid-filled cracks (Weertman, 1971; Secor & Pollard, 1975) indicates that a stable upward-rising crack can form from a magma source, driven by the density difference between the buoyant magma and overlying lithosphere. These models also suggest that the

Downloaded from http://petrology.oxfordjournals.org at Cambridge University on July 19, 2010

lithosphere should be in a state of tension, with one of the horizontal principal stresses being less than the vertical lithostatic stress.

Secor & Pollard (1975) give the following expression for $L_c$, the maximum stable length of a propagating fluid-filled crack (modified with symbols appropriate for present purposes),

$$L_c = 4(P_0 - \sigma_3)/g(\rho - \rho_m), \tag{4}$$

where $P_0$ is the representative magma pressure, $\sigma_3$ is the minimum stress, $\rho_m$ is the magma density, and $\rho$ is the mean density of the overlying lithosphere. For komatiitic liquids, the density contrast $(\rho - \rho_m)$ with a lithosphere of peridotite composition has been estimated to be in the range of 100 to 300 kg m$^{-3}$ (Nisbet & Walker, 1982). The source reservoir pressure $(P_0)$ for komatiite is assumed to reach values close to the lithostatic load and to be equal to the maximum principal stress. In the modern lithosphere, the deviatoric stress $(\sigma_1 - \sigma_3)$ has been estimated to range typically from 10 to 20 MPa (Solomon *et al.*, 1980). These ranges give crack lengths of tens to hundreds of kilometres, suggesting that it is reasonable to envisage pathways being created which provide a continuous but transient connection between source and surface. A continuous conduit between source and surface can be modelled by well-established relationships for open-channel flow (Wilson & Head, 1981).

Other plausible source conditions for komatiites are reservoirs of small volume or in which reservoir pressure decreases rapidly (Shaw, 1980). Such situations may not produce sufficient volume to create a continuous conduit. They would be anticipated to behave as buoyant magma-filled cracks, as envisaged by Weertman (1971) and Secor & Pollard (1975). Weertman's analysis suggests that such cracks have a stable length dependent on their volume and buoyancy. As such cracks ascend, they open at the top and close at the bottom. Weertman's analysis provides some approximate constraints on the volumes of magma that can be erupted from a single crack rising through a lithosphere of a given thickness. The vertical half-length of the crack is given by

$$L_c = [2AG/\pi(1-\sigma)g(\rho - \rho_m)]^{1/3}, \tag{5}$$

where $A$ is the cross-sectional area (m$^2$), $G$ is the shear modulus, and $\sigma$ is the Poisson's ratio. If the Archaean lithosphere was 50 km thick, the density contrast $(\rho - \rho_m) = 300$ kg m$^{-3}$, $G/(1-\sigma) = 9 \times 10^{10}$ newton m$^{-2}$ and $L_c = 25$ km (Nisbet & Walker, 1982), then the total volume for a fracture 10 km in horizontal length would be 8 km$^3$ of magma. Such calculations suggest that magma volumes less than a few km$^3$ will disconnect from their source and rise as a magma-filled crack.

The ascent of fluid-filled fractures is a complicated process involving considerations of the chemical and physical properties of both the host rock and the fluid (Anderson & Grew, 1977). Anderson (1978) has argued that magma intrusions are type II cracks, in which the crack propagation velocity is independent of the stress intensity at the crack tip, and is principally controlled by the ability of magma to flow into the region behind the tip. Two kinds of observations support this view. Firstly, acoustic waves are generated by cracks, but in the type I region of slow crack propagation (typically $v \ll 10^{-2}$ m s$^{-1}$), the velocities are too small to generate detectable seismicity. Dyke propagation is typically accompanied by seismic tremor (Aki *et al.*, 1977), which Anderson considers implies a viscosity-controlled crack growth. Secondly, the velocities of magma transport in propagating dykes recorded in the first rift zones of Kilauea and Krafla, Iceland, are from 0·3 to 0·5 m s$^{-1}$ (Pollard *et al.*, 1983). These velocities are similar to the velocities that would be expected for open-channel flow for basalt lavas of the observed viscosities moving in cracks of the observed dimensions. This suggests that the velocity is controlled by the fluid flow and that the behaviour of fluid in a confined crack does not depart substantially from an open conduit.

Downloaded from http://petrology.oxfordjournals.org at Cambridge University on July 19, 2010

If magma-filled cracks are primarily controlled by the ability of the fluid to move within the fracture, then komatiite ascent rates should be much faster than basalt, since komatiites have viscosities two or three orders of magnitude less than basalt. An open-channel analysis of flow is adequate despite the mechanical complexities of propagating cracks.

### *3c. Magma ascent rates*

At high Reynolds number, $Re$, the two-dimensional discharge rate, $Q$, from a long fissure of width, $d$, can be estimated as

$$Q = \left[\frac{g\Delta\rho}{k\rho_m}\right]^{1/2} d^{3/2}, \tag{6}$$

where $g$ is gravity, $\Delta\rho$ is the density contrast between the magma and the lithosphere overlying its source, $\rho_m$ is the magma density, and $k$ is a friction coefficient. The Reynolds number is defined as

$$Re = Q/v \tag{7}$$

where $v$ is the kinematic viscosity. Details of the Archaean lithosphere can only be adumbrated and a more rigorous treatment than that leading to (6) is not warranted. If the lithosphere is composed of peridotite, the value of $\Delta\rho$ is approximately 300 kg m$^{-3}$ at shallow depths, and could decrease to values of only 100 kg m$^{-3}$ at 100 km depth (Nisbet & Walker, 1982). The friction coefficient can be estimated from Schlichting (1960) for flow within a smooth conduit

$$k = 0{\cdot}32\, Re^{-0{\cdot}25}. \tag{8}$$

Typical values of $k$ lie between 0·01 to 0·04. Since conduits are unlikely to be hydraulically smooth, and the detailed shape is unknown, taking a value of $k = 0{\cdot}03$ is adequate. Magma density is assumed to be 2800 kg m$^{-3}$.

TABLE 3

*The two-dimensional flow rate, Q, the vertical velocity, v, and the Reynolds number, Re, in a fissure of width d assuming that the viscosity is 0·3 Pa s and the density 2800 kg m$^{-3}$*

| $d$ (m) | $Q$ (m$^2$ s$^{-1}$) | $v$ (m s$^{-1}$) | $Re$ |
|---|---|---|---|
| 0·3 | 0·56 | 1·9 | $5{\cdot}2 \times 10^3$ |
| 1·0 | 3·4 | 3·4 | $3{\cdot}2 \times 10^4$ |
| 3·0 | 17·8 | 5·9 | $1{\cdot}6 \times 10^5$ |
| 10·0 | 108 | 10·8 | $1{\cdot}0 \times 10^6$ |

Table 3 shows the variation of flow rate, $Q$, and ascent velocity with fissure width. The data imply typical ascent velocities of several metres per second and magma discharge rates of 0·5 m$^2$ s$^{-1}$ to approximately a hundred m$^2$ s$^{-1}$. If the horizontal length of the fissure was 1 km, then magma discharge rates would range from 500 to $10^5$ m$^3$ s$^{-1}$. These rates are larger than most eruption rates observed on a volcano like Hawaii (MacDonald, 1972), but comparable with eruption rates deduced from flood basalt provinces and lunar flows (Whitford-Stark, 1982).

Flows with Reynolds numbers in excess of 500 are fully turbulent. Fig. 2 shows the relationship between $Q$ and Reynolds number for magma viscosities in the range of 0·1 to

Downloaded from http://petrology.oxfordjournals.org at Cambridge University on July 19, 2010

10·0 Pa s. Using these viscosities as upper and lower ranges, it is evident from the diagram that nearly all komatiites will erupt as turbulent flows. The conditions for laminar flow are limited to crystal-rich komatiites erupting at rates below about a few $m^2\ s^{-1}$.

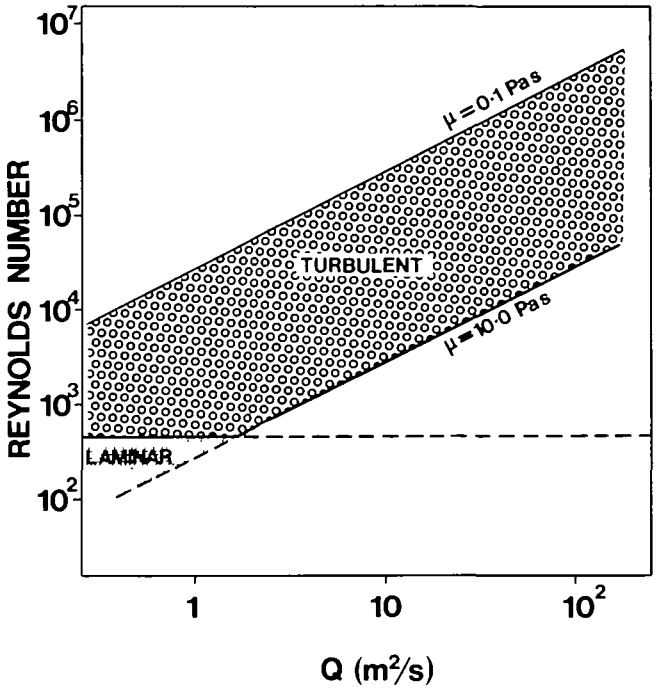


FIG. 2. The Reynolds number as a function of the two-dimensional flow rate, $Q$. Two lines of constant viscosity ($\mu = 0{\cdot}1$ and $\mu = 10{\cdot}0$ Pa s) are shown to cover the conditions of komatiite lavas. The regions of laminar flow conditions ($Re < 500$) and turbulent flow conditions are delineated.

### *3d. Lava eruption conditions*

Because of continuity, the flow rate in the fissure equals that along the ground. Therefore the Reynolds number just after eruption will not differ significantly from that in the fissure. Eruption processes, however, could lead to flow rates, and thereby Reynolds numbers, being somewhat greater in the lava than in the fissure. In many modern basaltic eruptions, activity begins along the entire length of a fissure, but quickly localizes to a few restricted positions. This is thought to occur by near-surface solidification of lava in the narrow parts and erosion of wider parts of the fissure system (Delaney & Pollard, 1982). Eruption from localized parts of a fissure would lead to higher values of the two-dimensional parameter $Q$ in the flow. The same kind of increase in $Q$ would be expected if the lava is channelled into a narrow pre-existing valley.

## 4. LAVA EMPLACEMENT

### *4a. Flow velocity and thickness*

We shall assume that the komatiite flowed in the form of a gravity current of high Reynolds number over a slope sufficiently small ($\ll 5°$) that its effects can be neglected. Komatiites are

Downloaded from http://petrology.oxfordjournals.org at Cambridge University on July 19, 2010

generally believed to erupt in submarine basins where slopes should be small. The flow thickness, $h$, can then be determined by the following expression after Britter & Simpson (1978)

$$h = (\tfrac{1}{2}Q^2\rho_m/g\delta\rho)^{1/3}, \tag{9}$$

where $\delta\rho$ represents the density difference, 1800 kg m$^{-3}$, between komatiite and seawater. Table 4 presents the flow thickness, $h$, velocity, $u$, and Reynolds number for different values of $Q$. A gravity current with a Reynolds number in excess of approximately 500 is fully turbulent. Our calculations (Table 4 and Fig. 2) indicate that this is the case for all komatiite lavas, whose velocities might have ranged between 2 and 10 m s$^{-1}$.

TABLE 4

*The lava flow thickness, h, its velocity, u, the Reynolds number, Re, as a function of the flow rate, Q, for a viscosity of 0·3 Pa s and a density of 2800 kg m$^{-3}$*

| $Q$ ($m^2$ $s^{-1}$) | $h$ ($m$) | $u$ ($m$ $s^{-1}$) | $Re$ |
|---|---|---|---|
| 0·5 | 0·27 | 1·8 | $4·7 \times 10^3$ |
| 1 | 0·43 | 2·3 | $9·3 \times 10^3$ |
| 10 | 1·99 | 5·0 | $9·3 \times 10^4$ |
| 100 | 9·26 | 10·8 | $9·3 \times 10^5$ |

### *4b. Theoretical analysis of cooling and thermal erosion*

Heat transfer is much greater in a turbulent flow than in a laminar flow, where heat is lost to the surroundings entirely by conduction. In turbulent flows, mixing maintains a uniform temperature throughout the span of the flow, and greatly enhances heat transfer to the surroundings. In turbulent flows, the ground surface would be quickly heated to temperatures of 1400–1650 °C. In greenstone belts, komatiites can sometimes flow over rocks, such as tholeiitic basalt, felsic volcanics and sediment (Lesher *et al.*, 1981; Arndt *et al.*, 1977; Gresham & Loftus-Hills, 1981), which have substantially lower melting temperatures, often by several hundreds of degrees centigrade. This leads to the suggestion that komatiites can melt and assimilate the ground (Fig. 3).

We adapt some of the theoretical treatment of Hulme (1973) to the turbulent flow and cooling of lava. Our model considers flow to occur on a shallow slope beneath a deep body of water. Both the ground and water are initially at temperature $T_0$, which is taken to be 0 °C. The heat transfer from the komatiite due to forced, turbulent convection melts some of the ground, which is swept along with the flow and assimilated within it. Above the flow, the efficient cooling by the water forms a thin crust on top of the lava and prevents any mixing between the lava and water. As the lava cools, crystals form within it which decrease the rate of cooling.

At steady-state the rate of the advance of the ground/lava interface (i.e. the melting rate) is given by (Hulme, 1973; Holman, 1976)

$$V = \frac{H}{\rho_g[c_g(T_m - T_0) + L_g]}, \tag{10}$$

where $H$ is the heat transfer rate to the ground, $\rho_g$ is the density of the ground, $T_m$ is the melting temperature of the ground, $c_g$ is the specific heat of the ground, and $L_g$ is the heat of

Downloaded from http://petrology.oxfordjournals.org at Cambridge University on July 19, 2010

the fusion of the ground. The heat transfer is related to $T_l$, the lava temperature, and $T_m$ through a heat transfer coefficient, $h_T$ (Holman, 1976), by

$$H = h_T(T_l - T_m) \equiv h_T \theta. \tag{11a, b}$$

An approximate value of the heat transfer coefficient can be obtained by modifying empirical relationships for turbulent pipe flows (Hulme, 1973; Holman, 1976)

$$h_T = 0{\cdot}02 \frac{k_l}{h} Pr^{0{\cdot}4} Re^{0{\cdot}8}, \tag{12}$$

where $k_l$ is the lava thermal conductivity and $Pr$ is the Prandtl number.

Huppert *et al.* (1984) made the simplifying assumptions that the melting temperature of the ground was equal to the solidus temperature of the komatiite, and that the viscosity and heat transfer coefficient were constant for a given flow. These assumptions were adequate to illustrate the general principles of rapid cooling and thermal erosion. However, in the general case the ground would not be expected to have the same melting temperature as the solidus temperature. Furthermore, both the viscosity and heat transfer coefficient will change downstream as the lava cools.

We consider the lava to freeze to form a crust at temperature $T_f$. Balancing heat fluxes through the top and base of the flow, then leads to

$$\rho_l c_l h \dot{\theta} = -2h_T \theta + h_T(T_f - T_m) - \frac{\rho_l c_l h_T \theta^2}{\rho_g [c_g(T_m - T_0) + L_g]} + \rho_l h L_x x'(T) \dot{\theta}, \tag{13}$$

where $\rho_l$ is the lava density, $c_l$ is the specific heat of the lava (assumed to be equal to that of the ground), $L_x$ is the heat of crystallization, and $x'(T) = \frac{1}{625}\,\mathrm{K}^{-1}$. The last term in equation (13) represents the effect of heat release due to crystallization and is derived from experimental studies of komatiite crystallization given in Arndt & Nesbitt (in press).

Manipulation of equation (13) leads to the following expression for the lava temperature $T_l$ as a function of downstream distance, $x$,

$$T_l = T_m + \gamma + \frac{(D + 2E\gamma)(\theta_0 - \gamma)}{(E\theta_0 + E\gamma + D)\exp[(D + 2E\gamma)x] - E(\theta_0 - \gamma)}, \tag{14}$$

where $\theta_0$ is the difference between the initial temperature of the lava at source ($x = 0$) and the melting temperature of the ground. The constants $D$, $E$ and $\gamma$ are given by

$$D = 2\tilde{h}_T/(\rho_l c_l Q) \tag{15}$$

$$E = \frac{\tilde{h}_T}{Q\rho_g [c_g(T_m - T_0) + L_g]} \tag{16}$$

$$\gamma = \tfrac{1}{2}[(D^2 + 4EF)^{\frac{1}{2}} - D]/E, \tag{17}$$

and

$$F = \frac{\tilde{h}_T(T_f - T_m)}{\rho_l c_l Q}, \tag{18}$$

and

$$\tilde{h}_T = h_T/[1 - L_x c_l^{-1} x'(T)], \tag{19}$$

where the subscripts g and l refer to the ground and lava respectively. We note that, when $T_f = T_m$, $\gamma = 0$ and equation (14) simplifies to the expression given by Huppert *et al.* (1984). Equation (14) is valid as long as the flow is turbulent ($Re > 500$), and the lava temperature is

Downloaded from http://petrology.oxfordjournals.org at Cambridge University on July 19, 2010

greater than the melting temperature. For flows cooler than the melting temperature ($T_l < T_m$), the following expression is valid for $Re > 500$

$$T_l = T_f + (T_m - T_f)\exp[-\tfrac{1}{2}D(x - x_m)], \tag{20}$$

where $x_m$ is the distance at which $T_l = T_m$ and is given by

$$x_m = \frac{1}{(D+2E\gamma)} \ln\left[\frac{(D+E\gamma)(\theta_0-\gamma)}{-\gamma(E\theta_0+E\gamma+D)}\right]. \tag{21}$$

The amount of ground assimilated as a volume fraction of the lava can be calculated from

$$S = \ln[(E\theta_0+E\gamma+D)e^{(D+2E\gamma)x} - E\theta_0 + E\gamma] - Dx - E\gamma x - \ln(D+2E\gamma). \tag{22}$$

### *4c. Results of theoretical analysis*

The values of the physical parameters used in the following calculations are listed in the table of symbols. We have modelled all flows with an initial temperature of 1600 °C, corresponding to an MgO content of approximately 30 per cent. We have chosen to illustrate the implications of different ground lithologies by discussing three reference rock types, whose assumed thermal properties are listed in Table 5. Archaean sediments from Kambalda, Western Australia, have average major element compositions similar to andesite (Bavinton, 1981) and are assumed to have the same thermal properties. In detail, each rock type will have a melting interval rather than a single melting temperature. We have taken the melting temperature to be the liquidus temperature, which therefore results in conservative calculations of melting rates and contamination effects.

TABLE 5

*Representative values of latent heat of fusion ($L_g$), melting temperature ($T_m$), and density ($\rho_g$) of Archaean rock types over which komatiite might have flowed*

| | $L_g$ ($J\ kg^{-1}$) | $T_m$ (°C) | $\rho_g$ ($kg\ m^{-3}$) |
|---|---|---|---|
| Tholeiitic basalt | $4{\cdot}2 \times 10^5$ | 1200 | 2700 |
| Sediment/andesite | $4{\cdot}2 \times 10^5$ | 1000 | 2500 |
| Acid gneiss | $3{\cdot}0 \times 10^5$ | 850 | 2300 |

Equation (14) has been used, together with equations (3) and (12), to calculate the variations of lava properties and contamination downstream. The calculations were carried out numerically, since the viscosity and heat transfer coefficients vary downstream. Results are presented for flow rates in the range 1 to 100 $m^2\ s^{-1}$.

*Length of thermal erosion channels*

The model envisages flow along a channel which deepens and slightly widens with time as the floor rocks are assimilated (Fig. 3). The one-dimensional theory allows quantitative assessment of the length and depth of thermal erosion channels. The width will be determined by other factors, such as the dimensions of the source vent or the occurrence of pre-existing channels.

Several factors limit the length of the lava channel influenced by thermal erosion. For situations where the melting temperature of the ground is less than or equal to the solidus

Downloaded from http://petrology.oxfordjournals.org at Cambridge University on July 19, 2010

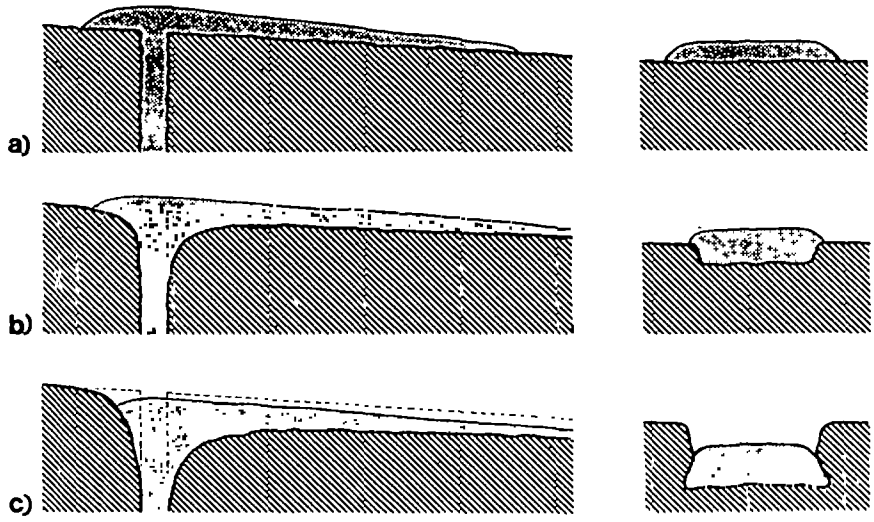


FIG. 3. Longitudinal and cross-sectional sketches of the fissure and lava flow, the melting of the ground, and formation of an erosional channel with time. The original ground surface and fissure width is indicated by dashed lines in (*b*) and (*c*).

temperature of the lava, the limit of thermal erosion will occur when the Reynolds number becomes subcritical. Laminar flow will occur beyond this distance, and thermal erosion will be negligible. Fig. 4*a* shows the distance at which the Reynolds number equals 500 for three different floor melting temperatures over a probable range of flow rates. For floor rocks with higher melting temperatures than the solidus temperature of the lava, another kind of limit can occur due to the lava becoming cooler than the floor melting temperature. This situation could occur, for example, where komatiite flows over another komatiite. Fig. 4*b* shows the distance over which assimilation can occur for $T_m = 1400\,^{\circ}C$. For flow rates above $3\ m^2\ s^{-1}$, the distance is controlled by the lava temperature decreasing to the ground melting temperature (equation (21)). For flow rates below $3\ m^2\ s^{-1}$, the distance is limited by transition to laminar flow when $Re = 500$.

Fig. 4 suggests that thermal erosion channels would typically be several to hundreds of kilometres in length. In practice, the length will also be limited by the dimensions and topography of the basins in which komatiites erupt. Thus for flow rates much greater than $10\ m^2\ s^{-1}$, komatiite lavas are likely to be ponded before the theoretical distance calculated here is attained. For reference, voluminous high flow rate eruptions of flood basalts and lunar basalts are generally ponded within major basins. Individual lavas in both these examples can be traced hundreds of kilometres and extended over areas comparable with the size of the basins envisaged for greenstone belts (Whitford-Stark, 1982).

*Erosion rates, channel depths, and slopes*

Fig. 5 shows the variation of melting rate in metres/day with distance from source for flow rates in the range 1 to $100\ m^2\ s^{-1}$ for the case $T_m = 1200\,^{\circ}C$. The curves show that for a fixed flow rate, the melting rate decreases downstream as the temperature of the lava decreases and the viscosity increases. A lower limit for melting rate occurs at the far end of the channel where the Reynolds number becomes subcritical. This limit is shown as a dashed curve. At a fixed distance downstream, the melting rate is an increasing function of the flow rate. This is

Downloaded from http://petrology.oxfordjournals.org at Cambridge University on July 19, 2010

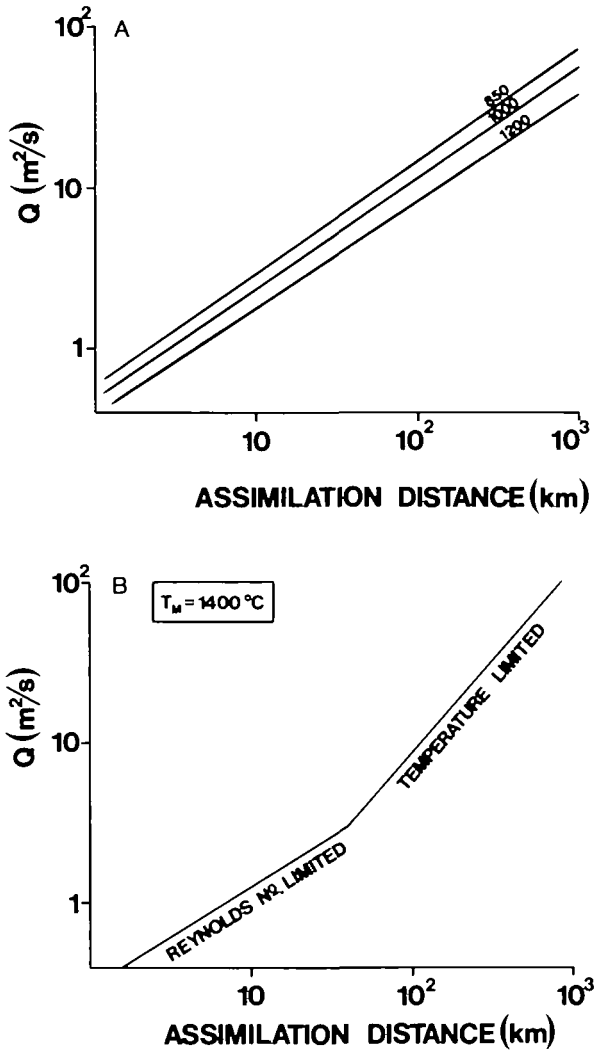


FIG. 4. A. The distance at which the Reynolds number reaches a value of 500 as a function of flow rate, $Q$. The lines are for three different floor melting temperatures in °C. This distance represents the limit of turbulent thermal erosion.

B. The distance at which significant thermal erosion will cease is shown as a function of flow rate, $Q$, for a floor with $T_m$ = 1400 °C. For flow rates greater than 3 $m^2 s^{-1}$, the distance corresponds to the location where the lava temperature has fallen below 1400 °C. For flow rates less than 3 $m^2 s^{-1}$, the distance corresponds to $Re$ = 500.

because a larger flow rate implies a larger value of the Reynolds number and hence a larger value of the heat transfer coefficient (see equation (12)). The largest melting rate occurs at source, where temperature difference is a maximum and the viscosity is a minimum. Fig. 6 shows the variation of initial maximum melting rate with flow rate and ground melting temperature. Figs. 5 and 6 together indicate that melting rates will typically range from 0·1 to 10 m $day^{-1}$, with enhanced rates for rocks with low melting temperatures.

From the calculated melting rates, the downstream shape of a channel can be calculated as a function of time. Fig. 7 shows a plot of channel depth versus distance for the case of $T_m$ = 1200 °C and $Q$ = 10 $m^2 s^{-1}$. Each curve represents a specific eruption duration. Results

Downloaded from http://petrology.oxfordjournals.org at Cambridge University on July 19, 2010

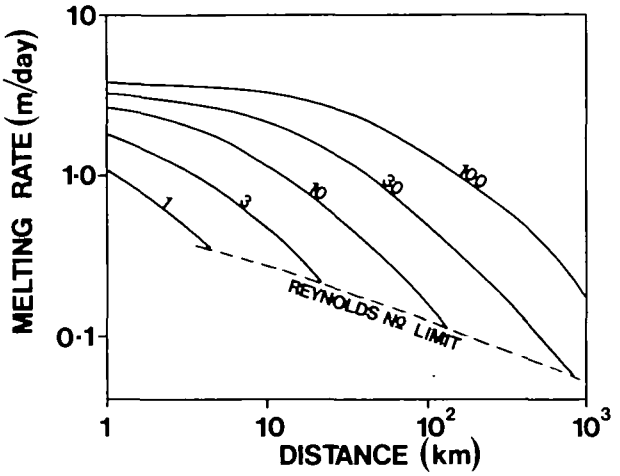


FIG. 5. Variation of melting rate with distance from source for different flow rates in $m^2 s^{-1}$ for $T_m = 1200\,°C$. The dashed line demarcates a value of $Re = 500$, beyond which the calculations are invalid and melting rates would become negligible.

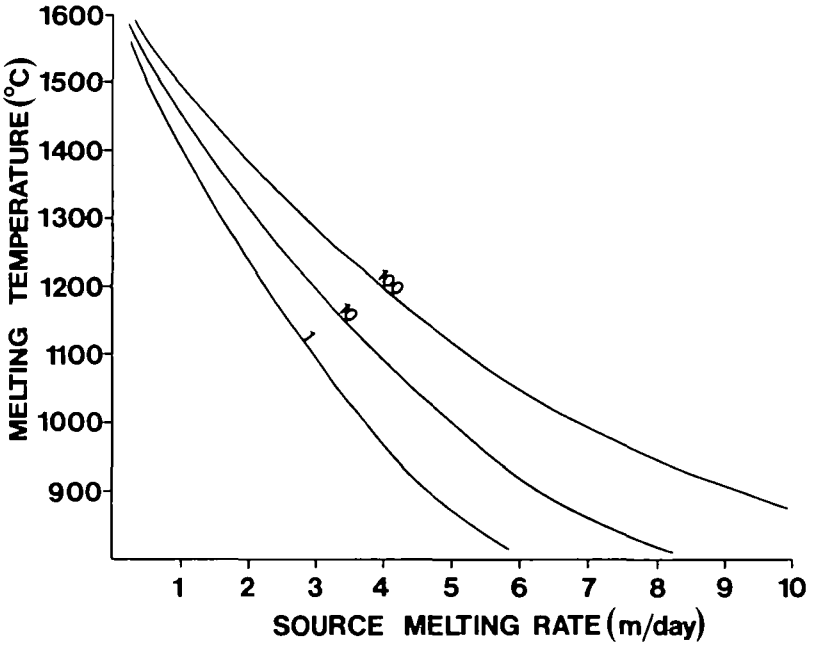


FIG. 6. Variation of melting rate at the source of the lava with melting temperature of the ground. Three curves are shown for flow rates of 1, 10 and 100 $m^2 s^{-1}$.

for other conditions all show similar shapes with the most vigorous erosion occurring in proximal regions. For those flows where the channel length is limited by a Reynolds number criterion (as in Fig. 5), the channel ends abruptly, although it is doubtful if real flows with fluctuating flow rates would form this feature.

The decrease of melting rate downstream will produce a change in gradient of the channel

Downloaded from http://petrology.oxfordjournals.org at Cambridge University on July 19, 2010

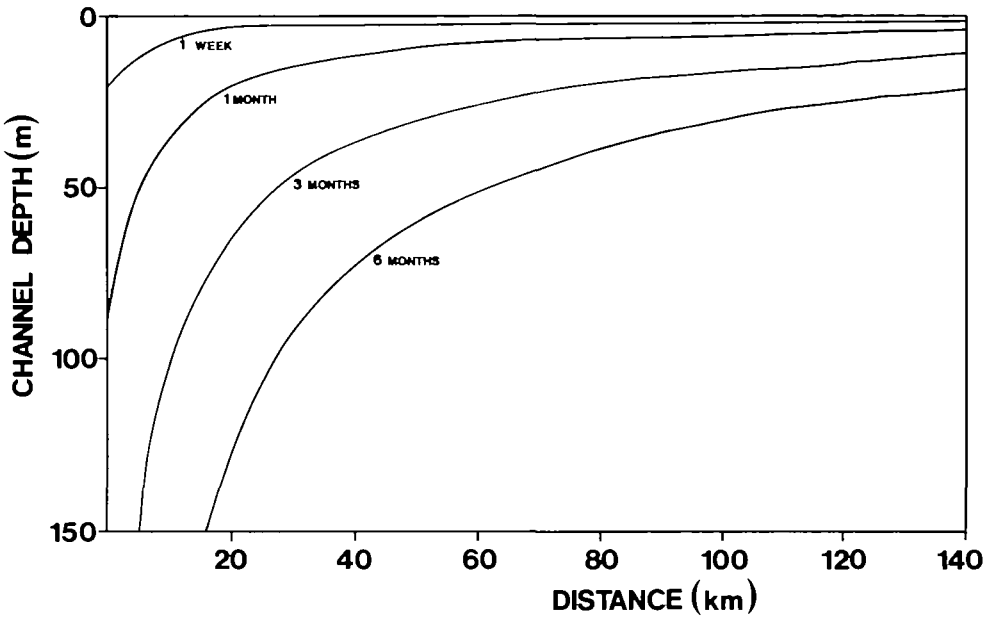


FIG. 7. Variations of channel depth *vs.* distance for a flow with $Q = 10\,m^2\,s^{-1}$ and $T_m = 1200\,°C$. The channel depth variation is shown for several durations of lava flowage down the channel.

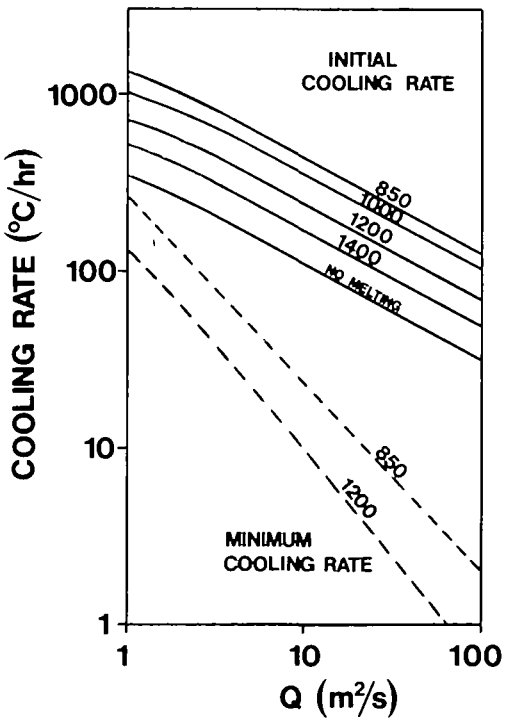


FIG. 8. The relationship between maximum cooling rate (°C $hr^{-1}$) and the flow rate for different values of the ground melting temperature (solid curves). The dashed curves show the calculated cooling rates at the point in a flow where $Re = 500$. Beyond this point the lava is no longer turbulent and interior cooling rates would decrease by several orders of magnitude.

Downloaded from http://petrology.oxfordjournals.org at Cambridge University on July 19, 2010

with time. On a horizontal surface, the gradient will develop towards the source vent. If komatiites erupted on to a horizontal or weakly-sloping sea floor, then the inverse slope of the channel could become a significant feature. The channel would become a confined linear feature in which the lava would become ponded, with a depth which decreases away from the source.

*Cooling rates and emplacement temperatures*

The turbulent flow conditions result in rapid cooling rates (equation (14)). Fig. 8 shows the variation of the (maximum) initial cooling rate at source with flow rate and ground melting temperature. Fig. 8 also shows the variation of cooling rate as a function of flow rate at the distal part of the turbulent flow, where $Re = 500$. Beyond this distance, the laminar condition of the flow reduces the cooling rate by orders of magnitude and thus this diagram shows the effective minimum cooling rate of a turbulent lava flow. These calculations indicate that cooling rates from a few to over a thousand °C per hour could characterize turbulent komatiite flows. Fig. 9 shows a typical result of the variation of temperature and cooling rate and contamination with distance from source for $Q = 10\,m^2\,s^{-1}$ and $T_m = 1200\,°C$ while the flow is turbulent. The results shown in this figure differ slightly from those presented by

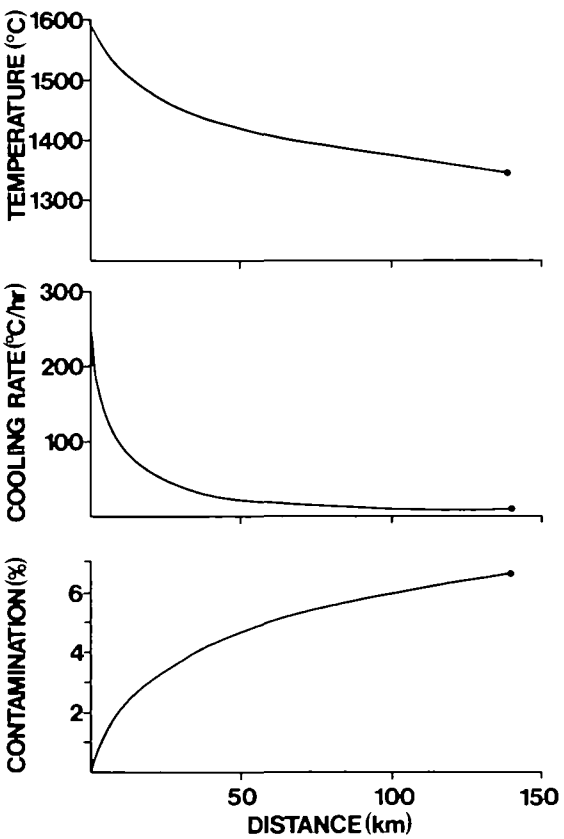


FIG. 9. Variation of temperature, cooling rate, and contamination with distance from source for a flow with $Q = 10\,m^2\,s^{-1}$ and $T_m = 1200\,°C$. The dot at the end of each curve represents $Re = 500$ and the solutions are invalid beyond this distance.

Downloaded from http://petrology.oxfordjournals.org at Cambridge University on July 19, 2010

Huppert *et al.* (1984) since the present solutions take into account the increase in viscosity with distance from the source, which has the effect of decreasing the cooling rate.

It is probable that after eruption many lavas were ponded in depressions. The emplacement temperature will depend on the distance to the nearest depression from the source. Our calculations indicate that lavas with large flow rates would remain turbulent for hundreds or thousands of kilometres. Since it is most unlikely that distances as great as these values exist to allow free flow, it is probable that many komatiites are ponded while still turbulent. For such flows an estimate of emplacement temperature can be made. Fig. 10*a* shows the emplacement temperature in a depression 100 km from the source for those flows which are still turbulent. The faster flows have higher emplacement temperatures.

*Contamination*

Fig. 9*c* shows the increase of contaminant with distance from source for $Q = 10\,m^2\,s^{-1}$ and $T_m = 1200$ °C. In general the maximum amount that can be assimilated is limited either by

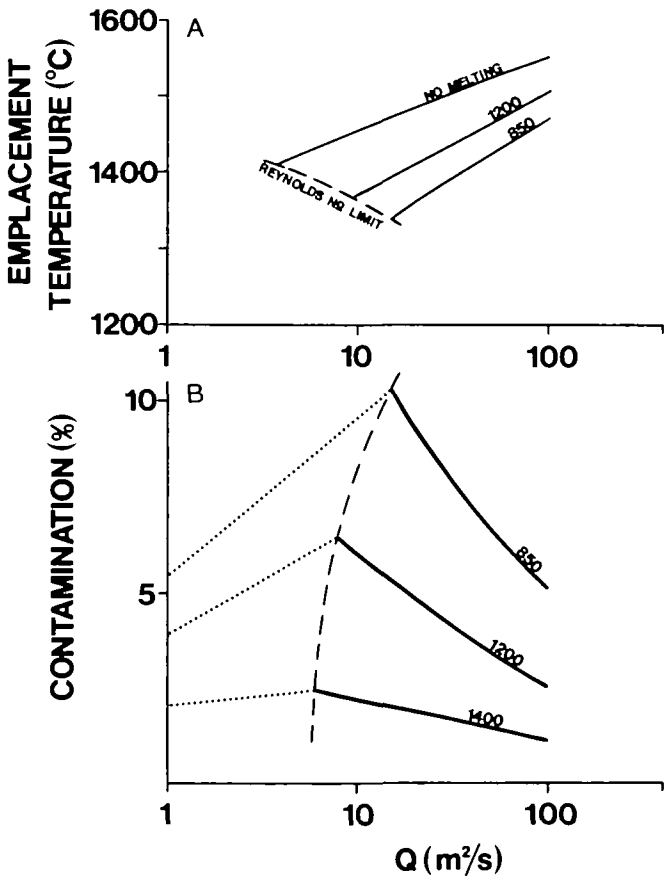


FIG. 10. A. Emplacement temperature *vs.* flow rate for the cases of no melting of the ground, $T_m = 1200$ °C and $T_m = 850$ °C for a lava emplaced at 100 km distance from source. The dashed line demarcates $Re = 500$ as the lava is emplaced and lavas with flow rates falling to the left of this line would not be capable of reaching a 100 km distance as turbulent flows.

B. Contamination in lavas *vs.* flow rate for the cases of $T_m = 1400$, 1200 and 850 °C for lavas emplaced at 100 km distance from source. The dashed line demarcates $Re = 500$ on emplacement and lavas to the left of this line would not be capable of reaching a 100 km distance as turbulent flows.

Downloaded from http://petrology.oxfordjournals.org at Cambridge University on July 19, 2010

the distance at which the Reynolds number becomes equal to 500, or by the lava temperature becoming less than the ground melting temperature. In most situations, the Reynolds number limit is the relevant factor. Fig. 11 shows the maximum amount of contamination as a function of flow rate and ground melting temperature. These calculations apply to a flow which reaches the assimilation limit without ponding. With large flow rates, the lava probably will pond well before this maximum is attained. Fig. 10*b* shows the amount of contamination expected in lavas which pond at 100 km distance. For sufficiently large flow rates the Reynolds number is still in excess of 500 beyond 100 km and the contamination decreases with increasing flow rate, and increases with lower melting ground temperatures.

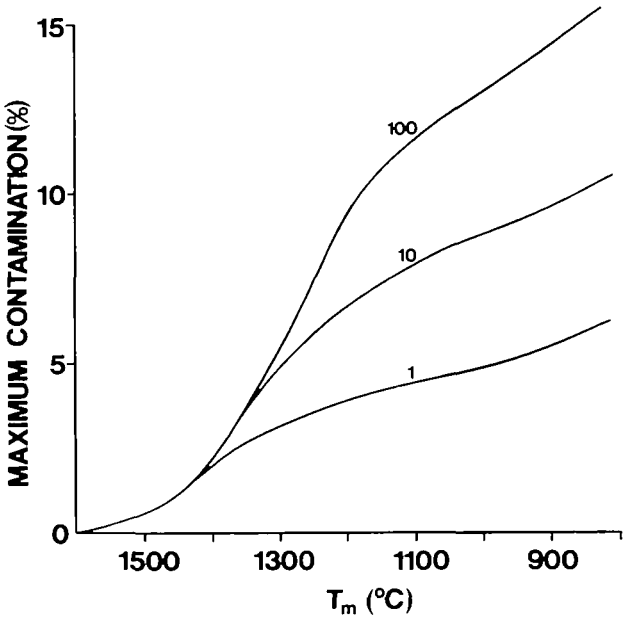


FIG. 11. The maximum contamination in a flow is plotted against ground melting temperature for three different flow rates: 1, 10, and 100 $m^2 s^{-1}$.

For slower flow rates, as indicated by the dotted curves, the Reynolds number has decreased below 500 before 100 km is attained; thermal erosion and further contamination will thus have ceased before the 100 km point is reached. The maximum contamination, as indicated by the dashed lines, is attained for flows where the Reynolds number is equal to 500 at the same distance as the ponding depression. Assuming that komatiites did not flow distances substantially greater than 100 km, these calculations suggest that about 10 per cent would be the practical upper limit for contamination. We note that komatiites could also become contaminated on ascent through Archaean crust. An investigation of thermal erosion during ascent is currently in progress.

*Crust formation*

Huppert *et al.* (1984) proposed that a thin crust forms on the flow surface as the lava chills against seawater. They calculated that crustal thicknesses of a few centimetres are likely to form during emplacement. The time scale, $\rho_l k_l L_x(T_F - T_0)/[\bar{h}_T(T_l - T_f)]^2$, for the crust to

Downloaded from http://petrology.oxfordjournals.org at Cambridge University on July 19, 2010

grow is quite short compared with the emplacement time of a lava, and suggests that a steady-state crust caps the flow.

Two factors may make the crust thinner than calculated. First, incandescent lava has been observed underwater (Moore, 1975), suggesting that quenching of the surface cannot be instantaneous. Mills (1984) has explained this phenomenon by the Leidenfrost effect in which, above a critical surface temperature, a layer of poorly conducting steam separates the lava from cold water. This effect enables the lava surface to remain incandescent for short periods. Second, the turbulent flow beneath may continually bring fresh hot lava to the surface and inhibit crust formation and allow the insulating sheath of steam to be maintained by keeping the surface temperature above the critical value. In these circumstances, heat loss from the upper surface will be by a combination of radiation and conduction through the film with no crust formation. Rapid cooling rates are qualitatively expected, but no analysis of this case is possible without information on the Leidenfrost temperature (Mills, 1984).

*Supersaturation effects*

The rapid cooling rates calculated here provide circumstances in which supersaturation and delayed nucleation of olivine crystals could occur. All the calculations presented thus far assume thermodynamic equilibrium, between crystals and melts, but experimental work (Donaldson, 1979) shows that at cooling rates of hundreds of degrees centigrade per hour, significant undercoolings and delayed nucleation are observed. Extrapolation of Donaldson's experimental data suggest undercoolings of 50–70 °C at cooling rates of several hundreds of °C per hour. For small flow rates, cooling rates in excess of $10^3$ °C $hr^{-1}$ have been calculated and, in some cases, there could be little crystallization during emplacement. Supersaturation effects would not be expected, however, if olivine crystals were already present on eruption and could act as nucleation sites. Table 6 compares the results of calculations neglecting crystallization completely and shows that cooling rates and melting rates increase for the case of no crystallization.

TABLE 6

*The cooling rate, $T(0)$, and the erosion rate at the source, $S(0)$, as a function of the flow rate, $Q$. The calculation assumes that $T_f = T_m = 1200$ °C. The values in parentheses represent the cases where no crystallization occurs and the latent heat effects are set equal to zero*

| $Q$ ($m^2\ s^{-1}$) | $T(0)$ (°C $hr^{-1}$) | $S(0)$ $m\ day^{-1}$ |
|---|---|---|
| 1 | 1300 (2730) | 3·33 (6·98) |
| 10 | 280 (590) | 3·33 (6·98) |
| 100 | 61 (127) | 3·33 (6·98) |

*4d. Laboratory experiments on thermal erosion*

A series of laboratory experiments were performed to investigate the processes involved in the formation of thermal erosion channels. Hot water at ≈ 65 °C was discharged at a variety of flow rates on to a smooth slab of polyethylene glycol (Peg 1000). This material melts at a temperature of 37–40 °C and is completely miscible with water. The slab had a slope of 2° in all the experiments.

In each experiment hot water was allowed to overflow from a container through a 1·5 cm wide entrance, which allowed the fluid to spread smoothly over the slab. In the early stages of

Downloaded from http://petrology.oxfordjournals.org at Cambridge University on July 19, 2010

each experiment, the water spread laterally and formed a sinuous stream which migrated laterally in an irregular manner across the slab (Fig. 12*a*). For the slower flows, the margins of the stream at this early stage were controlled by surface tension effects, which would not be important in lava flows. Melting and assimilation of the underlying slab occurred immediately, and within 30 seconds of the start of the experiment the flow had occupied a well-defined depression in the centre of the slab directly downslope of the entrance. In all experiments no further lateral migration occurred as the channel widened and deepened. Meanders in the channel, formed in the initial stages, were incised into the slab and maintained their initial curvature and position. There was a tendency for the channels formed at low flow rates to be more sinuous than those formed at high flow rates, which were straight-sided and preserved only gentle bends (Fig. 12*a*, *b*). A control experiment, in which water at room temperature flowed down the slab, led to a small amount of dissolution of polyethylene glycol. However, the rate of dissolution was negligible compared with the rate of thermal erosion observed in the main experiments.

The rate of thermal erosion was greatest near the source and decreased downstream (Fig. 12*c*) in agreement with theory. Two processes occurred which were not anticipated by the simple one-dimensional theory. Firstly, in each experiment the erosion rate was faster at the margins of the channel than at the centre. This resulted in a central ridge forming in the channel and a cross section as illustrated in Fig. 12*c*. Secondly, the walls of the channel became undercut and overhanging (Fig. 12*d*). This effect is a consequence of the flow only filling part of the channel depth and eroding both downwards and sideways at the margins. This latter effect could well be important in some komatiite lavas and could produce a channel with overhanging walls (Fig. 12*d*). Channels with shapes similar to those produced in the experiments have been observed in komatiites of Kambalda (Lesher, 1983; Lesher *et al.*, 1984). No quantitative studies of the experiments were undertaken, as we considered that measurements of temperatures and flow compositions could not be accurate enough to compare meaningfully with the theory.

### *4e. Comparison with lunar sinuous rilles*

A striking morphological feature of the lunar surface in the mare regions is the occurrence of long sinuous channels or rilles (Hulme, 1973, 1982). These channels are typically tens of kilometres long, hundreds of metres wide, and tens of metres deep. They range in shape from highly tortuous to relatively straight and parallel-sided channels. In some channels it can be demonstrated that the width and depth decrease systematically down slope (Head & Wilson, 1981). The channels are generally accepted to have formed by the flow of lava (Hulme, 1982).

Hulme (1973, 1982) proposed that the sinuous rilles are formed by thermal erosion. He calculated that the lunar flows were turbulent and had large volume flow rates. His calculations on thermal erosion of the lunar surface gave a typical initial erosion rate at source of 0·14 m per day. Head & Wilson (1981) have carried out further calculations based on Hulme's treatment and obtain source erosion rates of up to 1 m per day. These rates are less than we have calculated for the source rates of komatiite, because the lunar flows are thought to have lower eruption temperatures than komatiites and to have flowed over ground of similar composition. In order to form the observed dimensions of the rilles by thermal erosion, continuous flow over many months is required. This long duration is quite consistent with the large volumes of many mare lavas ($\approx 1000\ \mathrm{km}^3$) and estimated eruption rates (Wilson & Head, 1981; Head & Wilson, 1981). The shapes and dimensions of the rilles are consistent with both the quantitative and qualitative predictions of a thermal erosion model, as already argued in detail by Hulme (1982). Some lunar sinuous rilles may therefore be good analogies of the channels proposed to form in komatiite eruptions.

Downloaded from http://petrology.oxfordjournals.org at Cambridge University on July 19, 2010

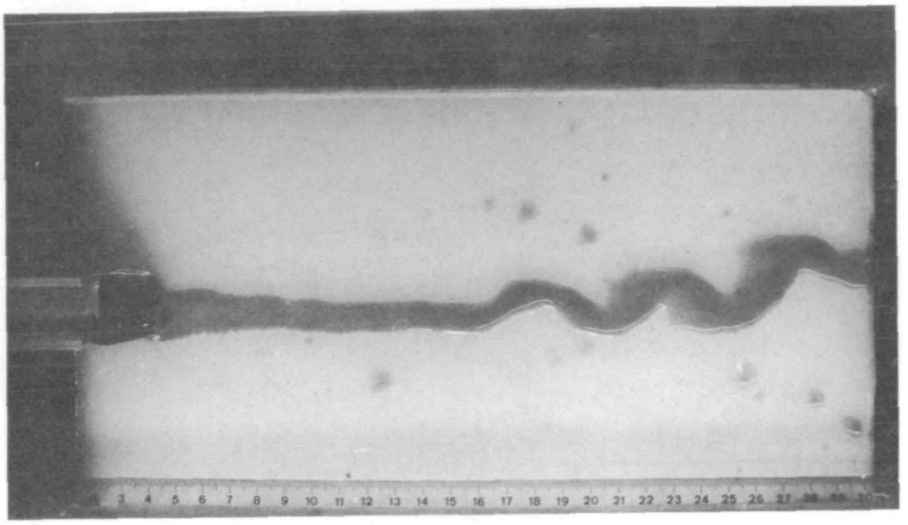

*a*

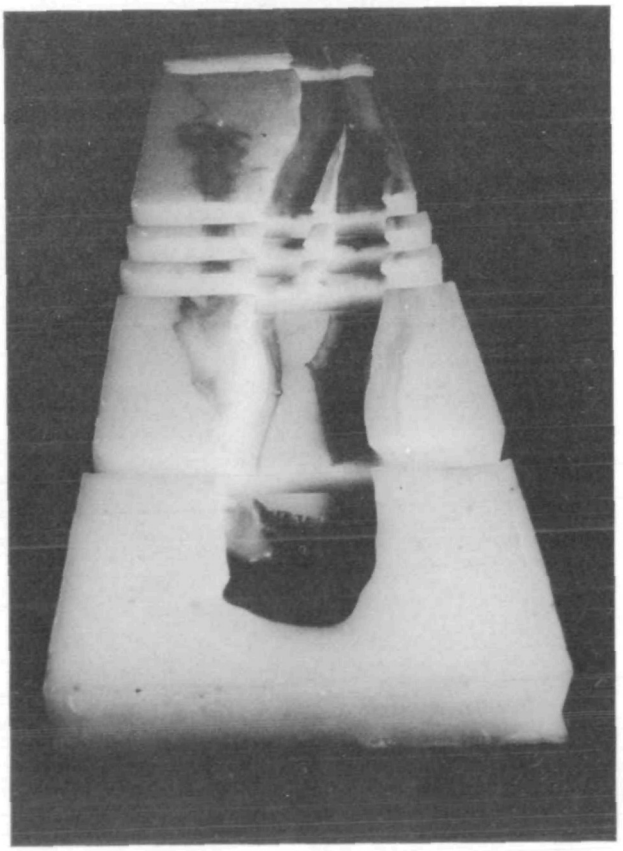

*b*

FIG. 12. Photographs of experiments simulating thermal erosion: (*a*) initial stages of an experiment in which a channel has yet to develop and the flow is highly sinuous and unsteady; (*b*) a well-developed channel is shown in plan-view preserving slight meanders;

[*continued overleaf*

Downloaded from http://petrology.oxfordjournals.org at Cambridge University on July 19, 2010

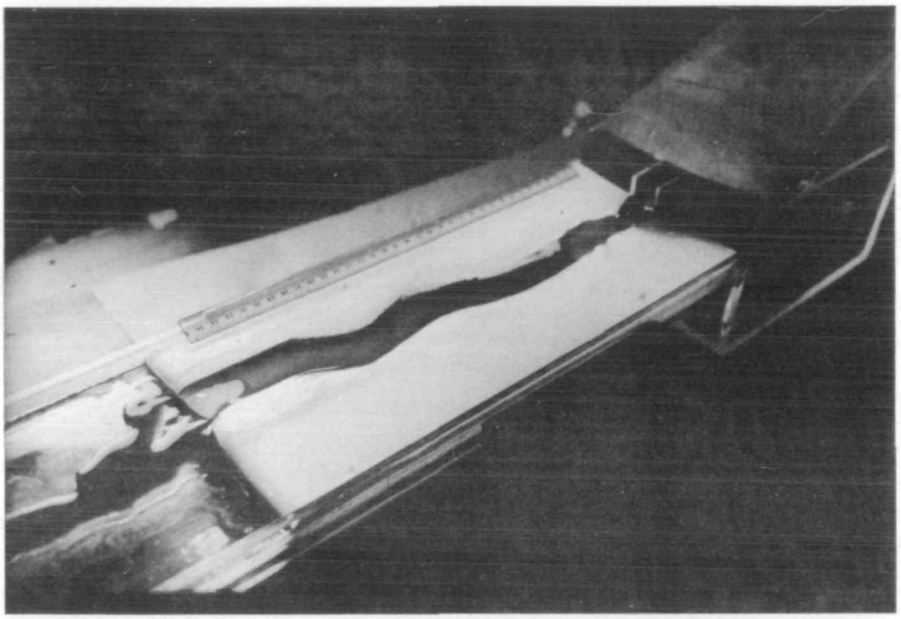

*c*

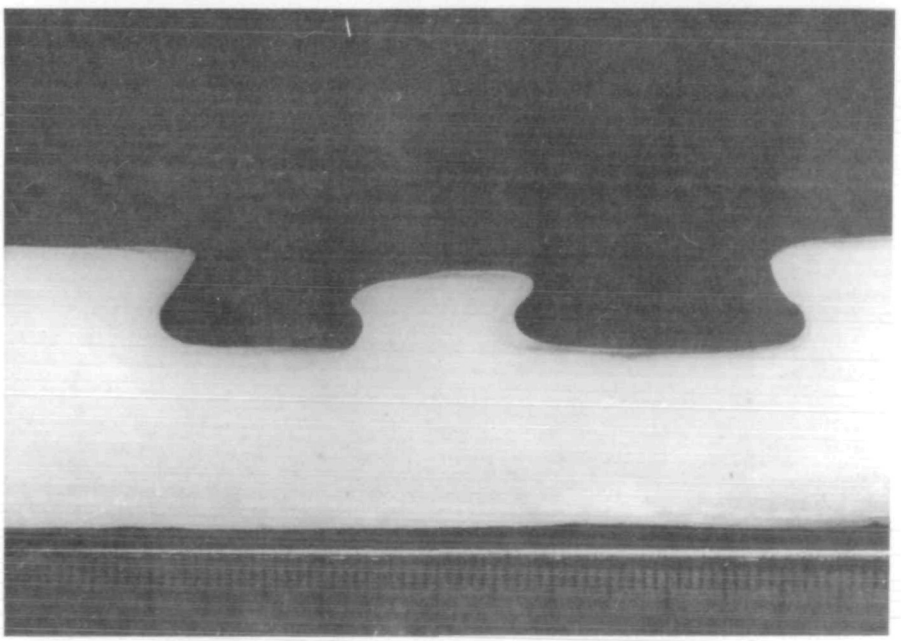

*d*

FIG. 12 (*continued*): (*c*) view of well-developed channel with decrease of channel depth evident downstream; (*d*) cross-section of an experimental channel.

Downloaded from http://petrology.oxfordjournals.org at Cambridge University on July 19, 2010

### *4f. Effects of olivine crystallization*

A process which might counteract thermal erosion is the sedimentation of olivine crystals from a flow to form an insulating layer of settled olivines on the floor of the lava channel. This section assesses whether olivine crystals would remain in suspension or sediment in komatiite flows.

The characteristic vertical component of velocity in the turbulent flow can be compared with the terminal settling velocity of olivine crystals. In a turbulent flow a characteristic velocity (sometimes known as the shearing stress velocity), is defined as

$$V_* = \beta(\tfrac{1}{2}k)^{\frac{1}{2}}u \tag{23}$$

where $\beta$ is a constant, $k$ is the friction coefficient, and $u$ is the flow velocity. Experiments (Jobson & Sayre, 1970; Gilette & Goodwin, 1974; Shreffler, 1975) show that if the shearing stress velocity is greater than the terminal fall velocity, dispersed solids remain in suspension. The constant $\beta$ has been found to vary from 0·12 to 0·65. The friction coefficient can be calculated from equation (8) in Section 3*e*.

With $\beta = 0{\cdot}3$ the shearing stress velocity of komatiite flows ranges from 8·7 to 29·6 cm $s^{-1}$ for flows with velocities from 2 to 15 m $s^{-1}$. Olivine crystals in the cumulate zones of komatiites from Munro Township have an approximate diameter of 0·1 cm (Pyke *et al.*, 1973), which is typical of many other lavas. Using Stokes Law, the settling velocities of such grains range from 12·3 cm $s^{-1}$ (at $\mu = 0{\cdot}1$ Pa s) to 0·013 cm $s^{-1}$ (at $\mu = 10$ Pa s). These values are much less than the calculated shearing stress velocities and indicate that olivines will remain in suspension in most flows. However, if the flow Reynolds number falls below 500, sedimentation can occur since turbulent motions are no longer present to suspend olivines.

## 5. GEOLOGICAL AND CHEMICAL IMPLICATIONS

### *5a. Field relationships*

The most conspicuous feature of the model is the formation of thermal erosion channels. The channels could be tens of metres deep and the komatiite would show clear cross-cutting relationships with underlying rock. However, the master feeding channels of lava flows, where appreciable thermal erosion might occur, may only occupy a small fraction of the total area covered by the lava. Initially, a lava may spread out over a wide area and channelization would become progressively more important with time. Lunar flows are instructive in this regard as the voluminous mare flows can cover enormous areas as wide and thin sheets, with significant thermal erosion being confined to the restricted narrow regions occupied by the rilles. On the flanks of a master channel and in distal areas, the lava would be emplaced as thin sheets with insufficient time for significant thermal erosion. We emphasize that thermal erosion is likely to be prominent only in channels through which there has been long-lived flow.

The komatiites of Kambalda, Western Australia, have been thoroughly investigated during exploration and exploitation of associated nickel-sulphide mineralization (Gresham & Loftus-Hill, 1981). The thickest and most richly mineralized komatiite unit rests stratigraphically over pillow basalts and thin sedimentary layers, in which striking elongate embayments are found. Detailed studies of these embayments (Lesher *et al.*, 1981; Lesher, 1983; Lesher *et al.*, 1984) provide convincing evidence that they represent contemporaneous channels. Individual embayments are tens of metres deep, hundreds of metres wide, and can sometimes be traced as troughs for at least 2 or 3 kilometres. The komatiite is significantly thicker in these embayments. Fig. 13 reproduces a cross-section of such an embayment after

Downloaded from http://petrology.oxfordjournals.org at Cambridge University on July 19, 2010

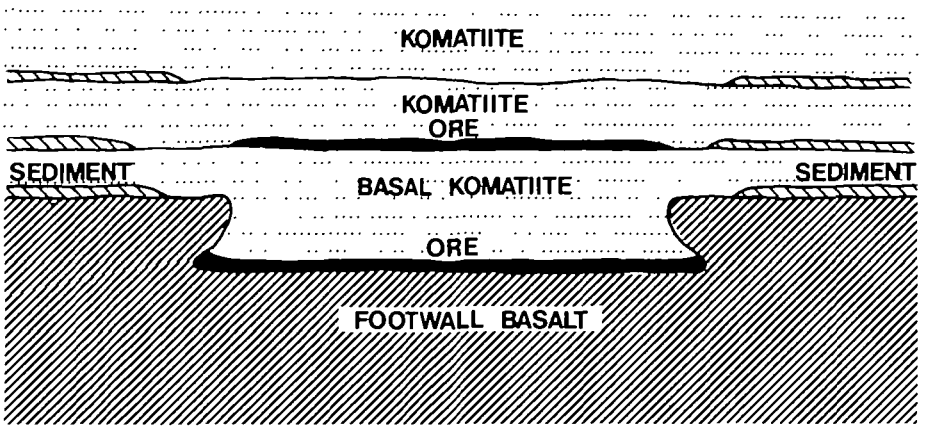


FIG. 13. Schematic reconstruction of the lithological contacts and rock units in the ore zones at Kambalda, Western Australia (modified after Lesher, 1983). No scale is shown as the thickness of units varies considerably. The embayments are typically tens of metres deep, a few hundred metres wide, and form long linear troughs in the third dimension. On the flanks of the embayment, the komatiite lava is considerably thinner and the sediments are a few metres thick.

Lesher (1983). Two striking features are the presence of overhanging walls of the underlying basalt and the absence of sediment in the structure.

We suggest that the geological relationships can be explained by the thermal erosion model. If channels with the preserved shape and relationships of those at Kambalda exist prior to komatiite emplacement, some problems emerge. One would expect the sediment layers to be thickest in a pre-existing channel, whereas they are in fact absent (Lesher *et al.*, 1984). It is also difficult to explain the apparent overhanging walls of the channels which would be unstable, although we note that folding and faulting could have been factors in forming this geometry (Gresham & Loftus-Hill, 1981; Lesher, 1983). Both these features can be explained by thermal erosion. The sediment is absent because the komatiite has eroded the sediment and incised deeply into underlying basalt. The overhanging walls of the channel margins are characteristic of our experimental channels. There is a close similarity between the experimental and geological cross-section (Figs. 12 and 13), although the latter was deduced by Lesher (1983) from independent geological evidence.

Other occurrences of komatiites, for example in the upper parts of the Kambalda succession and at Pyke Hill, Northern Ontario (Pyke *et al.*, 1973), show no evidence for erosion. In successions of thin units the base of one unit often rests on the glassy chilled top of another unit. These flows do not negate the model. They may have been emplaced rapidly as compound lava flows, or could represent flank or distal regions of a flow. Modern lavas can have complicated facies variations ranging from long-lived sustained flow in master channels to repeated and rapid emplacement of thin units in other areas. We suspect that individual komatiite flows will prove to be just as complicated.

### *5b. Internal layering and metastable crystallization*

The theoretical model proposed here supports and augments the view of Pyke *et al.* (1973) that the internal layering of komatiites is formed after emplacement. If crystallization occurs, the rapid cooling during flow and turbulent conditions could result in high nucleation rates. We suggest that many of the granular olivines are nucleated at the flow stage, but remain in suspension. The possibilities of sedimentation, except at the very end of flow, seem minimal.

Downloaded from http://petrology.oxfordjournals.org at Cambridge University on July 19, 2010

Some of our models also suggest that remarkably rapid cooling rates can occur, especially at low flow rates. At cooling rates of over 1000 °C per hr, for example, large supersaturations and long delays in nucleation can be anticipated. We suggest that there will be some flows which do not crystallize at all and are emplaced as strongly supersaturated melts. One consequence of emplacement of such a melt could be the sudden crystallization of skeletal olivine throughout the flow. Some komatiites have been described with randomly oriented spinifex throughout that can be explained by this mechanism. Examples of such flows were observed by one of us (RSJS) at Destor Township, Quebec. Another consequence could be the metastable crystallization of clinopyroxene, which apparently occurs in some flows, giving unexpected geochemical trends and orders of crystallization (Campbell & Arndt, 1982; Kinzler & Grove, in press). The main features of internal layering and differentiation, however, are thought to occur after emplacement and are discussed in detail in Part II.

### *5c. Trace element geochemistry*

Certain immobile trace elements, such as Zr, Ti, V, Y and Sc, appear to be resistant to various post-emplacement processes such as metasomatism, sea-floor alteration, and metamorphism. In addition, the ratios of these elements are not modified by fractional crystallization of olivine. Sun & Nesbitt (1977) have shown that the ratios of such elements are approximately chrondritic in many komatiites, but can show significant variation from flow to flow and from region to region. These variations in incompatible and immobile trace element ratios are often attributed to mantle heterogeneities.

Assimilation of underlying rock, as envisaged in the thermal erosion model, could also cause the observed variations in trace element ratios. This can occur because the rocks over which komatiite sometimes flows can have large absolute abundances of incompatible trace elements and ratios such as Zr/Y and Ti/Zr, which differ appreciably from those of komatiites. In these circumstances small amounts of contamination, well within the quantities indicated by the thermal erosion model, could cause shifts in the ratio comparable with those observed. Contamination is also likely during transport to the surface if komatiites ascend through Archaean continental crust. The effects of contamination will be similar to those discussed here.

We illustrate these effects using data from the Munro Township locality (Sun & Nesbitt, 1977; Arndt & Nesbitt, 1982). We chose this region because of the high quality and completeness of the geological and geochemical documentation. The Munro Township stratigraphy also suggests potential for contamination effects, since there is an intimate association of komatiites, komatiitic basalts, and Fe-rich tholeiites. We emphasize that our purpose is not to prove that contamination occurred at Munro Township. Mantle heterogeneity is an equally plausible explanation of the data. We merely wish to draw attention to the geochemical effects of thermal erosion and show that it could be significant.

Table 7 shows some representative calculations on the trace element variations that would occur in a komatiite flow moving over and assimilating an Fe-rich tholeiite. Composition (2) is based on data given by Arndt & Nesbitt (1982) for Pyke Hill komatiite. The starting composition has a REE pattern which is relatively depleted in light rare earths ($Ce_N/Yb_N \approx 0{\cdot}25$), and has low abundance of Zr, Y and Ti. Composition (1) is a Warden Town tholeiite which is in stratigraphic association with Munro Township komatiites. The basalt is light REE-enriched and has high contents of Zr, Y and Ti. The procedure of the calculations is to use the cooling assimilation model assuming that the basalt melts at 1200 °C and $Q = 10\ m^2\ s^{-1}$. The model is therefore a fractional crystallization model which is uniquely constrained by the conditions of cooling within the flow.

Downloaded from http://petrology.oxfordjournals.org at Cambridge University on July 19, 2010

TABLE 7

*Geochemical modelling of combined fractional crystallization and assimilation of komatiite lava (composition 2), which is progressively contaminated by an Fe-rich tholeiite (composition 1) downstream. Compositions 3–5 represent the calculated compositions of derivative liquids produced by olivine fractionation and assimilation. The relationship between temperature (T) and the amount of contamination (S) is calculated for $Q = 10\ m^2\ s^{-1}$ and $T_m = 1200\ °C$. The trace element values in parentheses represent the case of no assimilation and olivine fractionation. Data on compositions 1 and 2 from Arndt* et al. *(1977) and Arndt & Nesbitt (1982)*

| | *1* | *2* | *3* | *4* | *5* |
|---|---|---|---|---|---|
| $SiO_2$ | 51·87 | 47·24 | 49·03 | 50·92 | 52·40 |
| $TiO_2$ | 1·99 | 0·22 | 0·32 | 0·43 | 0·53 |
| $Al_2O_3$ | 12·82 | 4·10 | 5·40 | 6·73 | 7·89 |
| FeO | 14·83 | 10·49 | 11·87 | 12·60 | 12·97 |
| MgO | 5·04 | 30·30 | 24·60 | 19·14 | 13·97 |
| CaO | 6·44 | 5·84 | 7·40 | 8·94 | 10·28 |
| $Na_2O$ | 3·60 | 0·60 | 0·80 | 1·00 | 1·30 |
| *T* (°C) | | 1600 | 1500 | 1400 | 1300 |
| *S* (%) | | — | 2·5 | 5·6 | 8 |
| Zr | 138 | 14 | 20·7 (17·7) | 28·7 (21·6) | 36·2 (25·3) |
| Y | 48 | 8 | 11·1 (10·1) | 14·3 (12·3) | 17·1 (10·9) |
| $Ce_N$ | 20 | 1 | 1·73 (1·26) | 2·57 (1·54) | 3·26 (1·81) |
| $Yb_N$ | 12 | 4 | 5·23 (5·05) | 6·48 (6·16) | 7·61 (7·23) |
| Ti/Zr | 91 | 120 | 116 | 110 | 104 |
| Zr/Y | 2·88 | 1·75 | 1·86 | 2·0 | 2·11 |
| Ce/Yb | 1·66 | 0·25 | 0·33 | 0·4 | 0·43 |

Figs. 14 and 15 show geochemical plots of the trends expected by fractional crystallization of olivine and by combined olivine crystallization and assimilation of the tholeiitic basalt. Also plotted for comparison are various stratigraphic units of komatiite and komatiitic basalt found at Munro Township and documented by Arndt & Nesbitt (1982). The amount of assimilation is indicated at three points along the fractional crystallization/assimilation trend.

On a Ti versus MgO diagram (Fig. 14), the expected trend for olivine crystallization is rotated clockwise by contamination. Back projection of this trend to zero Ti content would not give the MgO content of the controlling olivine, and could give the spurious impression that orthopyroxene or some other MgO-poor phase was involved in magma genesis. The variation of Ti and Zr contents of the Munro Township lavas at a fixed value of MgO (Fig. 14 and Table 7) could be interpreted as due to mantle heterogeneity. However, inspection of the assimilation trend shows that the differences could also be produced by plausible amounts of assimilation of materials rich in Zr and Ti. A better match between the theoretical trends and observed spread of data, particularly for Zr, could be achieved by modifying the conditions of flow and composition of assimilated rock. For example, if we had chosen a Zr-rich felsic volcanic or acid gneiss with a lower melting point, greater enrichments in this element could be achieved. This would, however, be mere geochemical cookery, and would neither improve the argument nor prove that contamination was the actual process responsible.

The effect of assimilation on incompatible trace element ratios is clearest on a plot of Zr versus Ti/Zr (Fig. 15). Olivine crystallization would produce a horizontal trend with no change in this ratio, whereas for the particular calculation in Table 7, Ti/Zr is reduced quite markedly with decreasing Zr. There is a suggestion of a similar trend in the Munro Township

Downloaded from http://petrology.oxfordjournals.org at Cambridge University on July 19, 2010

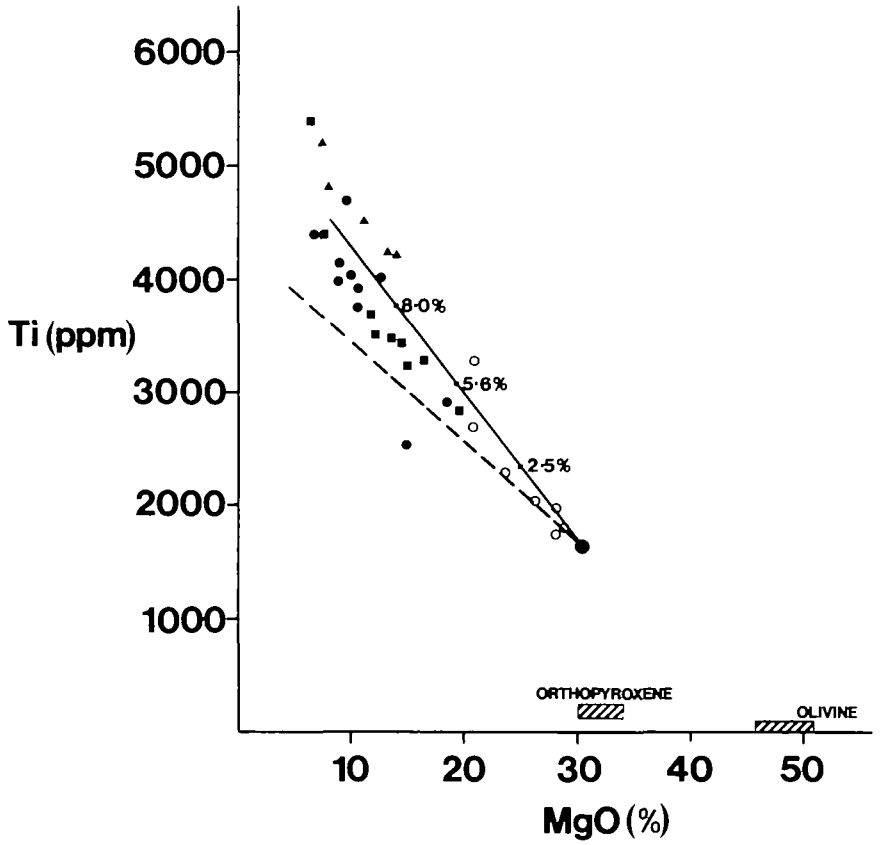


FIG. 14. Ti *vs.* MgO variation diagram. The dashed line shows the trend expected from fractional crystallization of olivine from composition 2 in Table 7 (marked as a large solid circle). The trend calculated during thermal erosion is due to combined assimilation and fractional crystallization. The points along the trend where 2·5, 5·6 and 8·0 per cent contamination has occurred is indicated. Calculations for this trend are detailed in Table 7. Data for Munro Township komatiites (open circles) and komatiitic basalts (solid symbols identical to those used by Arndt & Nesbitt, 1982) are also plotted. Each different solid symbol represents a different stratigraphic group of lavas.

lava data. Arndt & Nesbitt (in press) document petrographic and geochemical evidence for magma mixing between komatiite lavas and tholeiite at Munro Township. Such data could be just as validly interpreted as the consequence of assimilation (N. T. Arndt, pers. comm.).

REE patterns could be particularly affected by minor amounts of assimilation of appropriate material. A komatiite with initial $Ce_N/Yb_N$ equal to 0·25 would produce a basaltic komatiite with a flatter pattern ($Ce_N/Yb_N = 0{\cdot}43$) by assimilating tholeiitic basalt. More dramatically, contamination by material with $Ce_N = 50$, $Yb_N = 8$ and $Ce_N/Yb_N = 6{\cdot}25$ would produce a basaltic komatiite with a slightly enriched pattern ($Ce_N/Yb_N = 1{\cdot}3$). We emphasize that we have no doubt that mantle heterogeneity is an important and genuine phenomenon, which could well explain many variations. However, assimilation could be an important complicating factor in the interpretation of geochemical data from komatiites.

### *5d. Isotope geochemistry*

Dupré *et al.* (1984) studied the Pb and Nd isotope properties of two Archaean komatiites from Alexo, Ontario. A single flow showed sufficient variation in Sm/Nd to define an

Downloaded from http://petrology.oxfordjournals.org at Cambridge University on July 19, 2010

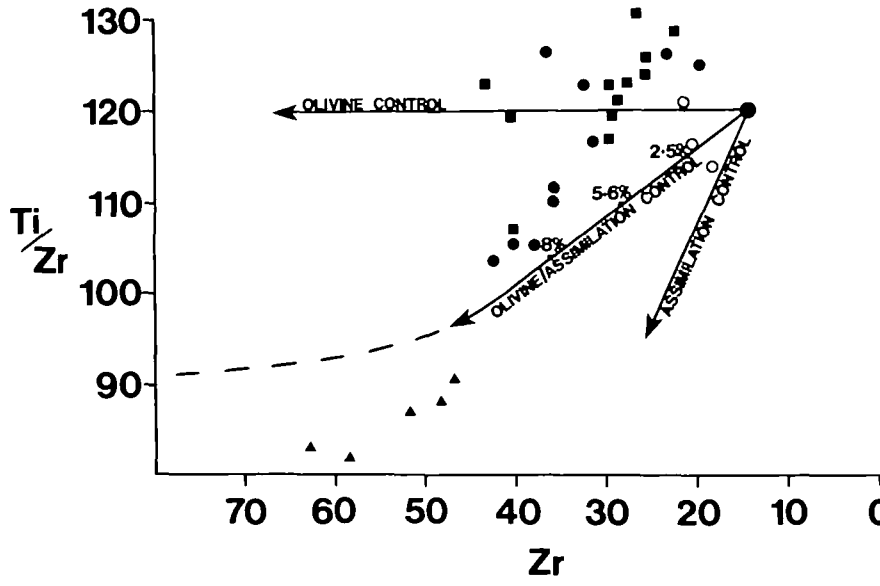


FIG. 15. Ti/Zr *vs.* Zr trends for calculations given in Table 7. The case of pure assimilation is also indicated. Symbols as in Fig. 14.

isochron and Dupré *et al.* argued that such variations could not be accounted for by olivine crystallization in the flow or later sea-floor alteration. The Sm/Nd ratio also correlates with Ti/Zr and $Al_2O_3$/Zr (N. T. Arndt, pers. comm.), which suggests that the effect is produced by igneous processes. Dupré *et al.* proposed two alternatives to explain these data. The first alternative is that the source changed during melting and on the time-scale of a single eruption; this is a possible but unlikely occurrence. The second alternative is that the flow assimilated the associated tholeiite with lower Sm/Nd to produce the observed scatter.

Thermal erosion could also produce isotopic heterogeneities in suites of komatiitic lavas, if the contaminant represents material of a different age (such as older gneisses) or lava derived from a different mantle source. In a suite of lavas which have been variably contaminated, a study of the Sm/Nd systematics could potentially yield an age greater than the eruption age. A discrepancy of 160 m.y. between U-Pb zircon ages and Sm/Nd whole rock ages have been reported by Cattell *et al.* (1984) from a komatiite suite in the Abititi Belt, Ontario. Thermal erosion could be an important process in modifying the Sm/Nd relationships and yielding older ages, as has recently been discussed by Bickle (1984).

### *5e. Nickel sulphide mineralization*

The arguments for interpreting some of the geological relationships at Kambalda as the consequence of thermal erosion have already been outlined. The model also provides an explanation for the origin of the sulphide mineralization, found confined to and at the base of the channels, by digestion of sulphur-rich sediment and basalt. Kambalda sediments now contain 3–7 per cent sulphur and originally contained greater amounts, up to 10 per cent, prior to metamorphism (Bavinton, 1981). Assimilation of up to 10 per cent sediment could potentially raise the sulphur content of the komatiite to 1 per cent, which is well above the amount required to saturate the melt in sulphide liquid (Skinner & Peck, 1969). An alternative and complementary mechanism of forming an immiscible sulphide liquid could arise from basalt assimilation. Cooling and assimilation of basalt would reduce the solubility

Downloaded from http://petrology.oxfordjournals.org at Cambridge University on July 19, 2010

of sulphur and cause the mixed fluid to enter into the field of sulphide saturation, as suggested by Irvine (1975) and Buchanan (in press).

The chalcophile element depletion trends at Kambalda are scattered, but are generally consistent with sulphide-saturated fractionation of olivine with olivine/sulphide ratios of approximately 100:1 or greater (Lesher *et al.*, 1981). The amount of sediment assimilation required to produce this ratio is in fact of the order of 3 per cent, which is easily achieved under most flow conditions. There is a great deal of geochemical data available on Kambalda sediments and komatiites. The geochemical evidence appears consistent with this model, although none can be itemized which gives positive evidence of assimilation. Unfortunately, the elements which would be most valuable for detecting sediment contamination are all susceptible to metamorphic modification (see also discussion by Lesher *et al.*, 1984). We consider that the geological evidence discussed in Lesher *et al.* (1984) provides the most persuasive arguments for the mineralization mode.

## ACKNOWLEDGEMENTS

Our interest in komatiites was stimulated by Nick Arndt during a visit to the Research School of Earth Sciences, Canberra, in 1982 and we acknowledge several stimulating discussions with him since. It is a pleasure to thank Mark Hallworth, who helped us with the experiments and preparation of the figures, and who is supported by the NERC. We also acknowledge fruitful discussions with Mike Bickle, Ian Campbell, Colin Donaldson, Ron Greeley, Mike Lesher, John Ludden, Dan McKenzie, Tony Naldrett, Bob Nesbitt, Ole Strecher, Stewart Turner and Lionel Wilson. We thank G. Urbain for useful correspondence concerning the viscosities of komatiite melts. Cliff Ford and Dan McKenzie provided careful reviews of an earlier version of this paper. Our research is generously supported by the BP Venture Research Unit. R.S.J.S. acknowledges support from the J. A. Tyrrell Burr Fund of the Geological Society to carry out field investigations of komatiites in Canada.

## REFERENCES

Aki, K., Fehler, M., & Das, S., 1977. Source mechanisms of volcanic tremor: fluid-driven crack models and their application to the 1963 Kilauea eruption. *J. Volcanol. geotherm. Res.* **2**, 259–88.

Anderson, O. L., 1978. The role of magma vapours in volcanic tremors and rapid eruptions. *Bull. volcan.* **41**, 341–53.

——& Grew, P. C., 1977. Stress corrosion theory of crack propagation with application to geophysics. *Rev. Geophys. Space Phys.* **15**, 77–104.

Arndt, N. T., Naldrett, A. J., & Pyke, D. R., 1977. Komatiitic and iron-rich tholeiite lavas of Munro Township, northeast Ontario. *J. Petrology*, **18**, 319–69.

——& Nesbitt, R. W., 1982. Geochemistry of Munro Township basalts. In: Arndt, N. T., & Nisbet, E. G. (eds.), *Komatiites*. Allen & Unwin, 309–29.

——————1985. Magma mixing in komatiitic lavas from Munro Township, Ontario, In: Hansen, G., Kroner, A., & Goodwin, A. W. (eds.) *Archean Geochemistry*. Springer-Verlag (in press).

Bagnold, R. A., 1966. An approach to the sediment transport problem from general physics. *Prof. Pap. U.S. geol. Surv.* **422-I**, 1–37.

Bavinton, O. A., 1981. The nature of sulfidic metasediments at Kambalda and their broad relationships with associated ultramafic rocks and nickel ores. *Econ. Geol.* **76**, 1606–28.

Bickle, M. J., 1982. The magnesium contents of komatiitic liquids. In: Arndt, N. T., & Nisbet, E. G. (eds.), *Komatiites*. Allen & Unwin, 479–94.

——1984. Are whole rock Sm/Nd ages suspect? *Nature*, **312**, 702–3.

——Ford, C. E., & Nisbet, E. G., 1977. The petrogenesis of peridotitic komatiites: evidence from high-pressure melting experiments. *Earth planet. Sci. Lett.* **37**, 97–106.

Bottinga, Y., & Weill, D. F., 1972. The viscosity of magmatic silicate liquids: a model for calculation. *Am. J. Sci.* **272**, 438–75.

Britter, R. E., & Simpson, J. E., 1978. Experiments on the dynamics of a gravity current head. *J. Fluid Mech.* **88**, 233–40.

Buchanan, D. L., 1985. Controls on the solubility of sulphur in mafic magmas. *Mineralium Deposita* (in press).

Campbell, I. H., & Arndt, N. T., 1982. Pyroxene accumulation in spinfex-textured rocks. *Geol. Mag.* **119**, 605–10.

Downloaded from http://petrology.oxfordjournals.org at Cambridge University on July 19, 2010

Cattell, A., Krough, T. E., & Arndt, N. T., 1984. Conflicting Sm–Nd whole rock and U–Pb zircon ages for Archean lavas from Newton Township, Abititi Belt, Ontario. *Earth planet. Sci. Lett.* **70**, 280–90.

Delaney, P. T., & Pollard, D. D., 1982. Solidification of basaltic magma during flow in a dike. *Am. J. Sci.* **282**, 856–85.

Donaldson, C. H., 1979. An experimental investigation of the delay in nucleation of olivine and mafic magmas. *Contr. Miner. Petrol.* **69**, 21–32.

Dupré, B., Chauvel, C., & Arndt, N. T., 1985. Pb and Nd isotopic study of two Archean komatiitic flows from Alexo, Ontario. *Geochim. cosmochim. Acta* (in press).

Gilette, D., & Goodwin, P. A., 1974. Microscale transport of sand-sized soil aggregates eroded by wind. *J. geophys. Res.* **79**, 4080–4.

Gresham, J. J., & Loftus-Hills, G. D., 1981. The geology of the Kambalda nickel field, Western Australia. *Econ. Geol.* **75**, 1373–416.

Head, G. W., & Wilson, L., 1981. Lunar sinuous rille formation by thermal erosion: eruption conditions, rates and durations. *Proc. Lunar planet. Sci. Conf.* **12**, 427–9.

Holman, J. P., 1976. *Heat Transfer*. McGraw-Hill.

Hulme, G., 1973. Turbulent lava flow and the formation of lunar sinuous rilles. *Modern Geology*, **4**, 107–17.

—— 1982. A review of lava flow processes related to the formation of sinuous rilles. *Geophysical Surveys*, **5**, 245–79.

Huppert, H. E., Sparks, R. S. J., Turner, J. S., & Arndt, N. T., 1984. The emplacement and cooling of komatiite lavas. *Nature*, **309**, 19–23.

Irvine, T. N., 1975. Crystallization sequences in the Muskox intrusion and other layered intrusions. II. Origin of chromitite layers and similar deposits of other magmatic ores. *Geochim. cosmochim. Acta*, **39**, 991–1020.

Jarvis, G. T., & Campbell, I. H., 1983. Archean komatiites and geotherms: solutions to an apparent contradiction. *Geophys. Res. Lett.* **10**, 1133–6.

Jobson, H. E., & Sayre, W. W., 1970. Vertical transfer in open channel flow. *Proc. Am. Soc. Civ. Engrs. Hydraul. Div.* **96**, 703–24.

Kinzler, R. J., & Grove, T. L., 1985. Crystallization and differentiation of Archean komatiite lavas from northeast Ontario: phase equilibrium and kinetic studies. *Am. Miner.* (in press).

Lesher, C. M., 1983. Localization and genesis of Fe-Ni-Cu sulphide mineralization at Kambalda, Western Australia. *Ph.D. thesis, University of Western Australia.*

—— Arndt, N. T., & Groves, D. I., 1984. Genesis of komatiite-associated nickel sulphide deposits at Kambalda, Western Australia: a distal volcanic-assimilation mode. Buchanan, D. L., & Jones, M. I. (eds.), I.M.M. Journal, *Proc. Nickel Sulphide Conf.* London, 70–80.

—— Lee, R. F., Groves, D. I., Bickle, M. J., & Donaldson, M. J., 1981. Geochemistry of komatiites from Kambalda, Western Australia: I. Chalcophile element depletion—a consequence of sulfide liquid separation from komatiitic magmas. *Econ. Geol.* **76**, 1714–28.

MacDonald, G. A., 1972. *Volcanoes*. New Jersey: Prentice-Hall, Inc.

McKenzie, D. P., 1984. The generation and compaction of partially molten rock. *J. Petrology*, **25**, 713–65.

Marsh, B. D., 1981. On the crystallinity, probability of occurrence, and rheology of lava and magma. *Contr. Miner. Petrol.* **78**, 85–98.

Mills, A. A., 1984. Pillow lavas and the Leidenfrost effect. *J. geol. Soc. Lond.* **141**, 183–6.

Moore, J. G., 1975. Mechanism of formation of pillow lava. *Am. J. Sci.* **6**, 269–77.

Nisbet, E. G., 1982. The tectonic setting and petrogenesis of komatiites. In: Arndt, N. T., & Nisbet, E. G. (eds.), *Komatiites*. Allen & Unwin, 501–20.

—— & Walker, D., 1982. Komatiites and the structure of the Archean mantle. *Earth planet Sci. Lett.* **60**, 103–13.

O'Hara, M. J., 1968. The bearing of phase equilibria studies in synthetic and natural systems on the origin and evolution of basic and ultrabasic rocks. *Earth Sci. Rev.* **4**, 69–113.

Pollard, D. D., Delaney, P. T., Duffield, W. A., Endo, E. T., & Okamura, A. T., 1983. Surface deformation in volcanic rift zones. *Tectonophysics*, **94**, 541–84.

Pyke, D. R., Naldrett, A. J., & Eckstrand, O. R., 1973. Archean ultramafic flows in Munro Township, Ontario. *Bull. geol. Soc. Am.* **84**, 955–78.

Ryan, M. P., Koyanagi, R. Y., & Fiske, R. S., 1981. Modeling three-dimensional structure of macroscopic magma transport systems: application to Kilauea Volcano, Hawaii. *J. geophys. Res.* **86**, 7111–29.

Schlichting, H. 1960. *Boundary Layer Theory*. New York: McGraw-Hill.

Secor, D. T., & Pollard, D. D., 1975. On the stability of open hydraulic fractures in the Earth's crust. *Geophys. Res. Lett.* **2**, 510–13.

Shaw, H. R., 1972. Viscosities of magmatic silicate liquids: an empirical method of prediction. *Am. J. Sci.* **272**, 870–93.

—— 1980. The fracture mechanisms of magma transport from the mantle to the surface. In: Hargraves, R. B. (ed.) *Physics of Magmatic Processes*. Princeton University Press, 201–64.

Shreffler, J. H., 1975. Numerical experimentation with particles having non-zero terminal velocity in the atmospheric surface layer. *Boundary-Layer Meteorol.* **9**, 191–204.

Skinner, B. J., & Peck, D. L., 1969. An immiscible sulphide melt from Hawaii. *Econ. Geol. Monogr.* **4**, 310–20.

Smith, H. S., & Erlank, A. J., 1982. Geochemistry and petrogenesis of komatiites from the Barberton greenstone belt, South Africa. In: Arndt, N. T., & Nisbet, E. G. (eds.), *Komatiites*. Allen & Unwin, 347–97.

Solomon, S. C., Richardson, R. M., & Bergman, E. A., 1980. Tectonic stress: models and magnitudes. *J. geophys. Res.* **85**, 6086–92.

Downloaded from http://petrology.oxfordjournals.org at Cambridge University on July 19, 2010

Sun, S. S., & Nesbitt, R. W., 1977. Chemical heterogeneity of the Archean mantle, composition of the Earth and mantle evolution. *Earth planet. Sci. Lett.* **35,** 429–48.

Ting, A. P., & Luebbers, R. H., 1957. Viscosity of suspensions of spherical and other isodimensional particles in liquids. *J. Am. Inst. Chem. Eng.* **3,** 111–16.

Urbain, G., Bottinga, Y., & Richet, P., 1982. Viscosity of liquid silica, silicates and alumino-silicates. *Geochim. cosmochim. Acta*, **46,** 1061–72.

Weertman, J., 1971. Theory of water-filled crevasses in glaciers applied to vertical magma transport beneath oceanic ridges. *J. Geophys. Res.* **76,** 1171–83.

Whitford-Stark, J. L., 1982. Factors influencing the morphology of volcanic landforms: an Earth–Moon comparison. *Earth Sci. Rev.* **18,** 109–68.

Wilson, L., & Head, J. W., 1981. Ascent and eruption of basaltic magma on the Earth and Moon. *J. geophys. Res.* **86,** 2971–3001.

Downloaded from http://petrology.oxfordjournals.org at Cambridge University on July 19, 2010